Presentazione

Questo documento è la versione compilata di un modello LaTeX di tesi di laurea o di dottorato, pronto all'uso, particolarmente indicato per lavori di carattere scientifico. Basato sul modello di Tesi Moderna proposto da Lorenzo Pantieri, è stato sviluppato per la stesura di tesi di laurea magistrale presso la Scuola di Ingegneria Industriale e dell'Informazione del Politecnico di Milano (PoliMi); esso risulta quindi immediatamente utilizzabile per tesi di Ingegneria al Politecnico di Milano, ma può essere impiegato con le opportune modifiche di layout anche in altre università. L'impianto LaTeX del modello di tesi (cartelle, files sorgente .tex, esempi di grafici e di database bibliografico) può essere scaricato al link indicato al termine di questa breve presentazione.

Agli Studenti del PoliMi

Le impostazioni di impaginazione sono state scelte con riferimento alle norme di stesura indicate dalla Facoltà di Ingegneria Industriale del Politecnico di Milano. Alcuni di questi parametri sono stati poi sostituiti o modificati per ottenere una resa tipografica più soddisfacente, senza allontanarsi però dalle principali linee guida indicate dal PoliMi; le impostazioni modificate possono essere facilmente ripristinate commentando/decommentando le relative righe di codice dei files sorgente.

Il frontespizio della prima pagina è stato creato con il pacchetto *frontespizio* e (purtroppo) non è quello ufficialmente previsto dal PoliMi. Il frontespizio "a norma" è quello che segue questa presentazione, e che apre inoltre il vero e proprio documento di tesi.

Nelle impostazioni iniziali vengono definiti i quattro colori ricorrenti del PoliMi, presenti anche nel tema delle presentazioni PowerPoint utilizzato dai docenti, che possono essere impiegati arbitrariamente all'interno del testo. Essi sono:

darkbluePoliMi	■
midbluePoliMi	■
lightbluePoliMi	■
orangePoliMi	■

A Tutti

Nel modello di tesi proposto i filetti delle tabelle e delle note a piè di pagina sono colorati in darkbluePoliMi, come visibile nella tabella sopra; lo scopo è quello di richiamare l'appartenenza all'università con finezze tipografiche che compariranno saltuariamente all'interno del testo. É estremamente semplice annullare questa

modifica all'interno del file ImpostazioniTesi.tex, o cambiare a piacimento il colore utilizzato (ad esempio gli studenti della Sapienza possono usare il Rosso Sapienza). A partire dai Link Utili tutto il testo colorato, all'interno del documento, è cliccabile.

Link Utili

Modello di tesi LaTeX completo e pronto all'uso:
link-modello-tesi-latex

Modello di Presentazione Powerpoint per Tesi di Laurea al Politecnico di Milano:
www.scribd.com

Script Matlab per inizializzare l'ambiente di lavoro e impostare le proprietà delle figure ottimali per la successiva inclusione nell'elaborato della Tesi e nella presentazione PowerPoint:
www.scribd.com

Mail – per segnalazioni, proposte e suggerimenti:
inviami-una-email

———————————————————

Materiale LaTeX sul sito web personale di Lorenzo Pantieri:
www.lorenzopantieri.net

Sito web del GuIT – Gruppo Utilizzatori Italiani di TeX e LaTeX:
www.guitex.org

Politecnico di Milano:
www.polimi.it

TeDOC – Servizio tesi e documentazione del Politecnico di Milano:
www.tedoc.polimi.it

POLITesi – Archivio digitale delle tesi di laurea e di dottorato del PoliMi:
www.politesi.polimi.it

POLITECNICO DI MILANO

Scuola di Ingegneria Industriale e dell'Informazione

Corso di Laurea Magistrale in
Physics Engineering

Modello di Tesi di Laurea in LaTeX

Relatore: Prof. Giacomo GHIRINGHELLI

Dott. Manuel SANCHEZ DEL RIO

Tesi di Laurea di:

Yiones AOUADI   Matr. 872727

Anno Accademico 2017 - 2018

Ringraziamenti

Lorem ipsum dolor sit amet, consectetuer adipiscing elit. Ut purus elit, vestibulum ut, placerat ac, adipiscing vitae, felis. Curabitur dictum gravida mauris. Nam arcu libero, nonummy eget, consectetuer id, vulputate a, magna. Donec vehicula augue eu neque. Pellentesque habitant morbi tristique senectus et netus et malesuada fames ac turpis egestas. Mauris ut leo. Cras viverra metus rhoncus sem. Nulla et lectus vestibulum urna fringilla ultrices. Phasellus eu tellus sit amet tortor gravida placerat. Integer sapien est, iaculis in, pretium quis, viverra ac, nunc. Praesent eget sem vel leo ultrices bibendum. Aenean faucibus. Morbi dolor nulla, malesuada eu, pulvinar at, mollis ac, nulla. Curabitur auctor semper nulla. Donec varius orci eget risus. Duis nibh mi, congue eu, accumsan eleifend, sagittis quis, diam. Duis eget orci sit amet orci dignissim rutrum.

Desidero inoltre ringraziare esplicitamente:

Esplicito1 per vari motivi;

Esplicito2 per altri motivi;

Esplicito3 per puro piacere, senza particolari motivi.

Milano, Dicembre 2018 L. M.

a te,
ovunque tu sia,
e qualunque percorso di vita tu abbia intrapreso.

Indice

Elenco delle figure

Elenco delle tabelle

Elenco dei codici

Sommario

Lorem ipsum dolor sit amet, consectetuer adipiscing elit. Ut purus elit, vestibulum ut, placerat ac, adipiscing vitae, felis. Curabitur dictum gravida mauris. Nam arcu libero, nonummy eget, consectetuer id, vulputate a, magna. Donec vehicula augue eu neque. Pellentesque habitant morbi tristique senectus et netus et malesuada fames ac turpis egestas. Mauris ut leo. Cras viverra metus rhoncus sem. Nulla et lectus vestibulum urna fringilla ultrices. Phasellus eu tellus sit amet tortor gravida placerat. Integer sapien est, iaculis in, pretium quis, viverra ac, nunc. Praesent eget sem vel leo ultrices bibendum. Aenean faucibus. Morbi dolor nulla, malesuada eu, pulvinar at, mollis ac, nulla. Curabitur auctor semper nulla. Donec varius orci eget risus. Duis nibh mi, congue eu, accumsan eleifend, sagittis quis, diam. Duis eget orci sit amet orci dignissim rutrum.

Nam dui ligula, fringilla a, euismod sodales, sollicitudin vel, wisi. Morbi auctor lorem non justo. Nam lacus libero, pretium at, lobortis vitae, ultricies et, tellus. Donec aliquet, tortor sed accumsan bibendum, erat ligula aliquet magna, vitae ornare odio metus a mi. Morbi ac orci et nisl hendrerit mollis. Suspendisse ut massa. Cras nec ante. Pellentesque a nulla. Cum sociis natoque penatibus et magnis dis parturient montes, nascetur ridiculus mus. Aliquam tincidunt urna. Nulla ullamcorper vestibulum turpis. Pellentesque cursus luctus mauris.

Parole chiave: PoliMi, Tesi, LaTeX, Scribd

Abstract

Text of the abstract in english. . .
Lorem ipsum dolor sit amet, consectetuer adipiscing elit. Ut purus elit, vestibulum ut, placerat ac, adipiscing vitae, felis. Curabitur dictum gravida mauris. Nam arcu libero, nonummy eget, consectetuer id, vulputate a, magna. Donec vehicula augue eu neque. Pellentesque habitant morbi tristique senectus et netus et malesuada fames ac turpis egestas. Mauris ut leo. Cras viverra metus rhoncus sem. Nulla et lectus vestibulum urna fringilla ultrices. Phasellus eu tellus sit amet tortor gravida placerat. Integer sapien est, iaculis in, pretium quis, viverra ac, nunc. Praesent eget sem vel leo ultrices bibendum. Aenean faucibus. Morbi dolor nulla, malesuada eu, pulvinar at, mollis ac, nulla. Curabitur auctor semper nulla. Donec varius orci eget risus. Duis nibh mi, congue eu, accumsan eleifend, sagittis quis, diam. Duis eget orci sit amet orci dignissim rutrum.

Nam dui ligula, fringilla a, euismod sodales, sollicitudin vel, wisi. Morbi auctor lorem non justo. Nam lacus libero, pretium at, lobortis vitae, ultricies et, tellus. Donec aliquet, tortor sed accumsan bibendum, erat ligula aliquet magna, vitae ornare odio metus a mi. Morbi ac orci et nisl hendrerit mollis. Suspendisse ut massa. Cras nec ante. Pellentesque a nulla. Cum sociis natoque penatibus et magnis dis parturient montes, nascetur ridiculus mus. Aliquam tincidunt urna. Nulla ullamcorper vestibulum turpis. Pellentesque cursus luctus mauris.

Keywords: PoliMi, Master Thesis, LaTeX, Scribd

Introduzione

Due esempi di pantografi in presa sono mostrati in figura 1; l'architettura asimmetrica del quadro (1b) è quella tradizionalmente adottata per i pantografi impiegati nell'alta velocità ferroviaria.

Argomento da Approfondire1

Qualche citazione. Lorem ipsum dolor sit amet, consectetuer adipiscing elit. Ut purus elit, vestibulum ut, placerat ac, adipiscing vitae, felis. Curabitur dictum gravida mauris. Nam arcu libero, nonummy eget, consectetuer id, vulputate a, magna. Donec vehicula augue eu neque. Pellentesque habitant morbi tristique senectus et netus et malesuada fames ac turpis egestas. Mauris ut leo. Cras viverra metus rhoncus sem. Nulla et lectus vestibulum urna fringilla ultrices. Phasellus eu tellus sit amet tortor gravida placerat. Integer sapien est, iaculis in, pretium quis, viverra ac, nunc. Praesent eget sem vel leo ultrices bibendum. Aenean faucibus. Morbi dolor nulla, malesuada eu, pulvinar at, mollis ac, nulla. Curabitur auctor semper nulla. Donec varius orci eget risus. Duis nibh mi, congue eu, accumsan eleifend, sagittis quis, diam. Duis eget orci sit amet orci dignissim rutrum.

Nam dui ligula, fringilla a, euismod sodales, sollicitudin vel, wisi. Morbi auctor lorem non justo. Nam lacus libero, pretium at, lobortis vitae, ultricies et, tellus. Donec aliquet, tortor sed accumsan bibendum, erat ligula aliquet magna, vitae ornare odio metus a mi. Morbi ac orci et nisl hendrerit mollis. Suspendisse ut massa. Cras nec ante. Pellentesque a nulla. Cum sociis natoque penatibus et magnis dis parturient montes, nascetur ridiculus mus. Aliquam tincidunt urna. Nulla ullamcorper vestibulum turpis. Pellentesque cursus luctus mauris.

(a) Architettura simmetrica (b) Architettura asimmetrica

Figura 1: Esempi di pantografi.

Figura 2: Nessuna immagine. . . Sorry.

Nulla malesuada porttitor diam. Donec felis erat, congue non, volutpat at, tincidunt tristique, libero. Vivamus viverra fermentum felis. Donec nonummy pellentesque ante. Phasellus adipiscing semper elit. Proin fermentum massa ac quam. Sed diam turpis, molestie vitae, placerat a, molestie nec, leo. Maecenas lacinia. Nam ipsum ligula, eleifend at, accumsan nec, suscipit a, ipsum. Morbi blandit ligula feugiat magna. Nunc eleifend consequat lorem. Sed lacinia nulla vitae enim. Pellentesque tincidunt purus vel magna. Integer non enim. Praesent euismod nunc eu purus. Donec bibendum quam in tellus. Nullam cursus pulvinar lectus. Donec et mi. Nam vulputate metus eu enim. Vestibulum pellentesque felis eu massa.

E adesso una nota a piè di pagina.[1] In figura 2 non è riportata alcuna immagine. . . o forse si?

Scopi della Tesi

Lorem ipsum dolor sit amet, consectetuer adipiscing elit. Ut purus elit, vestibulum ut, placerat ac, adipiscing vitae, felis. Curabitur dictum gravida mauris. Nam arcu libero, nonummy eget, consectetuer id, vulputate a, magna. Donec vehicula augue eu neque. Pellentesque habitant morbi tristique senectus et netus et malesuada fames ac turpis egestas. Mauris ut leo. Cras viverra metus rhoncus sem. Nulla et lectus vestibulum urna fringilla ultrices. Phasellus eu tellus sit amet tortor gravida placerat. Integer sapien est, iaculis in, pretium quis, viverra ac, nunc. Praesent eget sem vel leo ultrices bibendum. Aenean faucibus. Morbi dolor nulla, malesuada eu, pulvinar at, mollis ac, nulla. Curabitur auctor semper nulla. Donec

---

[1]Nota a piè di pagina.

varius orci eget risus. Duis nibh mi, congue eu, accumsan eleifend, sagittis quis, diam. Duis eget orci sit amet orci dignissim rutrum.

Nam dui ligula, fringilla a, euismod sodales, sollicitudin vel, wisi. Morbi auctor lorem non justo. Nam lacus libero, pretium at, lobortis vitae, ultricies et, tellus. Donec aliquet, tortor sed accumsan bibendum, erat ligula aliquet magna, vitae ornare odio metus a mi. Morbi ac orci et nisl hendrerit mollis. Suspendisse ut massa. Cras nec ante. Pellentesque a nulla. Cum sociis natoque penatibus et magnis dis parturient montes, nascetur ridiculus mus. Aliquam tincidunt urna. Nulla ullamcorper vestibulum turpis. Pellentesque cursus luctus mauris.

Nulla malesuada porttitor diam. Donec felis erat, congue non, volutpat at, tincidunt tristique, libero. Vivamus viverra fermentum felis. Donec nonummy pellentesque ante. Phasellus adipiscing semper elit. Proin fermentum massa ac quam. Sed diam turpis, molestie vitae, placerat a, molestie nec, leo. Maecenas lacinia. Nam ipsum ligula, eleifend at, accumsan nec, suscipit a, ipsum. Morbi blandit ligula feugiat magna. Nunc eleifend consequat lorem. Sed lacinia nulla vitae enim. Pellentesque tincidunt purus vel magna. Integer non enim. Praesent euismod nunc eu purus. Donec bibendum quam in tellus. Nullam cursus pulvinar lectus. Donec et mi. Nam vulputate metus eu enim. Vestibulum pellentesque felis eu massa.

Outline

Il testo della tesi è così strutturato:

Nel primo capitolo è delineato lo stato dell'arte Lorem ipsum dolor sit amet, consectetuer adipiscing elit. Ut purus elit, vestibulum ut, placerat ac, adipiscing vitae, felis. Curabitur dictum gravida mauris. Nam arcu libero, nonummy eget, consectetuer id, vulputate a, magna. Donec vehicula augue eu neque. Pellentesque habitant morbi tristique senectus et netus et malesuada fames ac turpis egestas. Mauris ut leo. Cras viverra metus rhoncus sem. Nulla et lectus vestibulum urna fringilla ultrices. Phasellus eu tellus sit amet tortor gravida placerat. Integer sapien est, iaculis in, pretium quis, viverra ac, nunc. Praesent eget sem vel leo ultrices bibendum. Aenean faucibus. Morbi dolor nulla, malesuada eu, pulvinar at, mollis ac, nulla. Curabitur auctor semper nulla. Donec varius orci eget risus. Duis nibh mi, congue eu, accumsan eleifend, sagittis quis, diam. Duis eget orci sit amet orci dignissim rutrum.

Il secondo capitolo presenta i risultati della campagna di prove sperimentali Nam dui ligula, fringilla a, euismod sodales, sollicitudin vel, wisi. Morbi auctor lorem non justo. Nam lacus libero, pretium at, lobortis vitae, ultricies et, tellus. Donec aliquet, tortor sed accumsan bibendum, erat ligula aliquet magna, vitae ornare odio metus a mi. Morbi ac orci et nisl hendrerit mollis. Suspendisse ut massa. Cras nec ante. Pellentesque a nulla. Cum sociis natoque penatibus et magnis dis parturient montes, nascetur ridiculus mus. Aliquam tincidunt urna. Nulla ullamcorper vestibulum turpis. Pellentesque cursus luctus mauris.

Nel terzo capitolo si descrivono le scelte di modellazione Nulla malesuada porttitor diam. Donec felis erat, congue non, volutpat at, tincidunt tristique, libero. Vivamus viverra fermentum felis. Donec nonummy pellentesque ante. Phasellus adipiscing semper elit. Proin fermentum massa ac quam. Sed diam turpis, molestie vitae, placerat a, molestie nec, leo. Maecenas lacinia. Nam ipsum ligula, eleifend at, accumsan nec, suscipit a, ipsum. Morbi blandit ligula feugiat magna. Nunc eleifend consequat lorem. Sed lacinia nulla vitae enim. Pellentesque tincidunt purus vel magna. Integer non enim. Praesent euismod nunc eu purus. Donec bibendum quam in tellus. Nullam cursus pulvinar lectus. Donec et mi. Nam vulputate metus eu enim. Vestibulum pellentesque felis eu massa.

Capitolo 1

Focusing for X-rays

"Terence: Rotta a nord con circospezione
Bud: Ehi, gli ordini li do io qui!
Terence: Ok, comante
Bud: Rotta a nord
Terence: Soltanto?
Bud: Con circospezione!"

Chi Trova un Amico Trova un Tesoro

L'introduzione deve essere atomica, quindi non deve contenere nè sottosezioni nè paragrafi nè altro. Il titolo, il sommario e l'introduzione devono sembrare delle scatole cinesi, nel senso che lette in quest'ordine devono progressivamente svelare informazioni sul contenuto per incatenare l'attenzione del lettore e indurlo a leggere l'opera fino in fondo. L'introduzione deve essere tripartita, non graficamente ma logicamente:

1.1   Introduction

Image formation usually implies some form of focusing. How this focusing occurs depends on the way in which the radiation interacts with its surroundings. Thus for visible light the well-known laws of reflection and refraction are utilized, while, while electrons are caused to travel in curved paths in electromagnetic field. X-rays interact with matter in three ways (each causing attenuation of the X-ray beam): elastic scattering, inelastic scattering, and absorption via the photoelectric effect. Elastic scattering (in which exchange of energy is involved) is caused by two process: Thomson scattering from single atomic electrons, and Rayleigh (or coherent) scattering, which occurs from strongly bound electrons acting cooperatively. The scattered and incident beams have a ddefinite phase relationship and interference can occour (Bragg diffraction). Inelastic, incoherent, or Compton scattering occurs from loosely bound (essentialle free) electron and involves the transfer of a small fraction of the energy of an incident X-ray photon. The scattered and incident beams do not have fixed relationship, and the atom is raised to a different quantum state due to the excitation of the electron. Absorbtion (through the photoelectric effect) occurs when the X-ray photon transfer all its energy to an inner atomic

electron, thereby releasing it from atom (ionization)

In Figure 1 the linear attenuation coefficient for these processes are plotted as functions of energy for two materials, carbon and gold, important in soft X-ray physics. For the soft X-ray regime

1.2 Interaction with Matter

When a beam of electromagnetic radiation passes through a material, the intensity is exponentially attenuated

$$I = I_0 exp(-\alpha x) \tag{1.1}$$

where x is the thickness of the material, α is the linear attenuation coefficient, and I_0 is the intensity at $x = 0$. The amplitude of the electromagnetic wave at x is

$$A = A_0 exp(\frac{-2\pi\beta x}{\lambda}) exp(\frac{-2\pi i(nx - ct)}{\lambda}) \tag{1.2}$$

where λ is the vacuum wavelength of the radiation, n is the refractive index of the material, and β is its absorption coefficient. The complex refractive index of the material, which governs the propagation of the electromagnetic wave is

$$\overline{n} = n - i\beta \tag{1.3}$$

Since, at soft X-ray wavelengths, absorption is the dominant process, α may be identified with a linear absorption coefficient, where

$$\alpha = \frac{4\pi\beta}{\lambda} \tag{1.4}$$

Tabulation of X-ray absorption data usually give the mass absorption coefficient μ, where

$$\alpha = \mu\rho \tag{1.5}$$

and ρ is the density of the material. The mass absorption of a compound is given by

$$\mu_{\text{com}} = \sum_j w_j \mu_j \tag{1.6}$$

where w_j is the weight fraction of the constituent with mass absorption coefficient μ_j. The linear absorption coefficient of the compound is then

$$\alpha_{\text{com}} = \mu_{\text{com}}\rho_{\text{com}} \tag{1.7}$$

where ρ_{com} is the density of the compound.

In the X-ray region, the energies of individual photons are much larger than the binding energies of outer atomic electron (typically a few electron volts) and molecular binding energies. Absorbing atoms are therefore ionized by the radiation and most of the energy is transferred to the kinetic energy of ejected electron. The energy of an X-ray photon may only be absorbed by an atomic electron from the state. Thus, as the X-ray energy increase, the absorption coefficient will undergo several relatively sharp increases (absorption edges) at energies corresponding to binding energies of different atomic levels. as shown in Figure 1. In practice these increases are not so sharp as indicated, because of the finite energy widths of atomic states and because of the environment of the absorbing atoms.
The theoretical treatment of X-ray scattering and absorption has been given in detail by many authors. A brief summary is included here because the results have implication for the design of X-ray optical system. The starting point of the calculation is to consider the scattering of X rays by free electron (Thomson scattering). An electro-magnetic wave whose electric vector has amplitude A_0 causes such an electron (of charge e and mass m_e) to be accelerated by an amount $A_0(e/m)$. Accelerated charges radiate, the amplitude of the electric vector at a distance r from the charge being

$$A_T(\Phi) = \frac{e}{4\pi\varepsilon_0 c^2 r} a \sin\Phi \tag{1.8}$$

where Φ is the angle between the direction $\mathbf{r}$ and the acceleration $\mathbf{a}$. Thus

$$A_T(\Phi) = A_0 \frac{e^2}{4\pi\varepsilon_0 c^2 r} \sin\Phi \tag{1.9}$$

To describe the interaction of an electromagnetic wave with an electron bound in an atom, the Thomson amplitude $A_T(\Phi)$ is multiplied by a complex atomic scattering factor $f_1 + if_2$, so that the scattered amplitude is given by

$$A(\Phi, E) = A_T(\Phi)[f_1(E) + if_2(E)] \tag{1.10}$$

where the factor f_1 and f_2 depend on the energy E of the incoming radiation but it is assumed that, to a first approximation, they do not depend on the scatting angle ϑ (i.e. the angle between the incoming and scattered radiation). This assumption is valid since the wavelengths of interest ($\sim 1 - 10nm$) are larger to typical dimension of the atomic electron distribution ($\sim 1 - 50pm$) so that the atomic electrons may be considered to scatter in phase. The factor f_1 and f_2 can be calculated in relativistic quantum dispersion theory and are given by

$$f_1(E) = Z + 4\frac{\varepsilon_0 m_e c}{he^2} \int_0^{+\infty} \frac{W^2 \sigma(W)}{E^2 - W^2} dW - \Delta_{(}rel) \tag{1.11}$$

and

$$f_2(E) = 2\frac{\varepsilon_0 m_e c}{h} E\sigma(E) \tag{1.12}$$

The first term in the equation 1.11 describes Thomson scattering (Z is the atomic number of scatterer) and, to describe the angular dependence of the scattering, may be replaced by the angle-dependent form factor

$$f0 = \int_0^{+\infty} U(r) sinc[\frac{4\pi r}{\lambda} \sin\frac{\vartheta}{2}] dr \tag{1.13}$$

where $U(r)$ is the radical charge distribution and $sinc(x) = \frac{\sin x}{x}$. If the wavelength λ is in nanometres, then for $\sin\frac{\vartheta}{2} \leq \frac{\lambda}{2}$, $f_0 = Z$, while for $\sin\frac{\vartheta}{2} = \lambda$, $f_0 \simeq 0.9Z$ for most elements.

The second term in 1.11, the anomalous dispersion integral, is the same as that given semiclassically by considering the electrons to be caused to oscillate by the incoming radiation, Because it neglects damping, this term results in imprecise values for f_1 close to absorption edges. The atomic photo ionization cross section $\sigma(E)$ (in $m^2 atom^{-1}$) is related to the mass absorption coefficient by

$$\sigma(E) = A\frac{\mu}{N_0} \tag{1.14}$$

where A is the atomic weight and N_0 is Avogadro's number. In order to calculate $\sigma(E)$ theoretically the atomic wave function must be know; these have to be obtained by approximation methods for all system excepts hydrogen, leading to to uncertainties in the expressions for f_1 and f_2.

The third term in equation 1.11 is a relativistic correction, which is negligible at X-ray energies (except near absorption edges) to assume that the solid state environment does nor greatly affect the ionization process, since it is the outer atomic levels that are most modified when an atom is bound in a solid. Then, the atomic parameters f_1 and f_2 may be related to macroscopic factors n and β by

$$\delta = 1 - n = \frac{e^2\hbar^2}{2\varepsilon_0 m_e E^2}\overline{f_1} \tag{1.15}$$

and

$$\beta = \frac{e^2\hbar^2}{2\varepsilon_0 m_e E^2}\overline{f_2} \tag{1.16}$$

where f_1 and f_2 are the average atomic scattering factors per unit volume,

$$\overline{f_1} = \sum jN_jf_{1j} \qquad \overline{f_2} = \sum jN_jf_{2j} \tag{1.17}$$

and N_j is the number of atoms of type j per unit volume. For energies well away from any absorption edges, equation 1.15 reduces to

$$\delta = \frac{Ne^2\hbar^2}{2\varepsilon_0 E^2} = \frac{Ne^2\lambda^2}{8\pi^2\varepsilon_0 m_e c^2} \tag{1.18}$$

where N is the total number of electrons per unit volume. This equation 1.18, is the same as that originality derived by Lorentz using classical ideas of absorption. In X-ray region, δ is small (typically $\sim 10^{-3}$) and positive, i.e., the refractive index for soft X rays is slightly less than unity. Tables of values for f_1 and f_2 have been published, and these were used to generate Figure 1, along with the experimentally observed variation of the absorption coefficient away from an absorption edge:

$$\beta \sim Z^2\lambda^3 \tag{1.19}$$

1.3   Total External Reflection

The propagation of X rays in matter may be described by the complex refractive index

$$\overline{n} = n - i\beta = 1 - \delta - i\beta \tag{1.20}$$

where δ is small and positive. Thus the real part of the refractive index is, unlike the case for visible light, less than one and so, if a normal refractive lens were to be usef for focusing, it would habe ti ve concave to give a real focus for an incident plane wave. For a plano-concave lens with central thickness d (Figure 1.19)

$$\frac{f}{\rho} = 1 + \frac{n}{\cos\varphi - n\cos\varphi'} \tag{1.21}$$

where f is the focal length, ρ is the radius of curvature of the concave surface, and φ and φ' are the anlges with respect to the normal to the concave surface as defined in Figure 2. For axial rays, this becomes

$$\frac{f}{\rho} = 1 + \frac{n}{1-n} = \frac{1}{\delta} \tag{1.22}$$

The depth of focus of such a lens is given by

$$\Delta f = \pm \frac{1}{2} \left(\frac{f}{r} \right)^2 \lambda \tag{1.23}$$

where r is the radius of the lens aperture and λ is the illuminating wavelength. The maximum thickness of lens is, form Figure 2 ,

$$t = \rho - (\rho^2 - r^2)^{\frac{1}{2}} + d \tag{1.24}$$

The closeness of the refractive index to unity, and the high absorption of soft X rays, means that lenses of the same sort of dimensions as those used for visible light would have impossibly long focal length ($\geq 10m$), very small depths of focus ($\sim$tens of micrometers), and they would absorb essentially all of the incident radiation. Thus this type of lens s impractical for X ray, as has been started by previous authors.

However, optical components currently in use for X rays can have focusing effective of about 10% and effective aperture radii of about $10 - 50\mu m$. To match this this efficiency, a refractive lens should have a mean thickness such that about 10% of the incident intensity is transmitted. Two possible lenses, for soft-X ray wavelength of about $3.5nm$, are shown in Table 1. These results show that such lenses may nor be unreasonable, although they have very large f-number and so very intense source would be needed to prevent long imaging times. Calculation for biconcave lenses give similar results. However, the exact focusing property of soft X-ray refractive lenses depend on a better knowledge than currently available for the optical constants, and to date no attempts have been made to manufacture them.

The other conventional method of focusing at visible wavelengths is to use refractive optics. The reflected amplitude, a, at an interface between vacuum and a material is given by the Fresnel equation. For radiation polarized so that the electric vector is perpendicular to the plane of incidence (s polarization)

$$a_\perp = \frac{\cos \varphi - (\overline{n}^2 - \sin^2 \varphi)^{\frac{1}{2}}}{\cos \varphi + (\overline{n}^2 - \sin^2 \varphi)^{\frac{1}{2}}} \tag{1.25}$$

where the angle of incidence φ is measured from the surface normal. In terms of the glancing angle, $\vartheta = 90° - \varphi$, this becomes

$$a_\perp = \frac{\sin \vartheta - (\overline{n}^2 - \cos^2 \vartheta)^{\frac{1}{2}}}{\sin \vartheta + (\overline{n}^2 - \cos^2 \vartheta)^{\frac{1}{2}}} \tag{1.26}$$

For parallel polarized radiation (p polarization)

$$a_\parallel = \frac{\overline{n}^2 \sin \vartheta - (\overline{n}^2 - \cos^2 \vartheta)^{\frac{1}{2}}}{\overline{n}^2 \sin \vartheta + (\overline{n}^2 - \cos^2 \vartheta)^{\frac{1}{2}}} \tag{1.27}$$

The reflectivity is given by

$$R = \frac{I}{I_0} = aa^* \tag{1.28}$$

where I_0 is the incident intensity and I is the reflected intensity. For radiation incident normally on a surface, $\vartheta = 90°$ and equations 1.26 and 1.27 both lead to the normal incident reflectivity

$$R_n = \left(\frac{1 - \overline{n}}{1 + \overline{n}}\right)^2 = \frac{\delta^2 + \beta^2}{(2 - \delta)^2 + \beta^2} \tag{1.29}$$

Using the values given in Table 1, and equation 1.4, gives, for a wavelength of $3.5nm$, $R_n = 3.3x10^{-6}$ for carbon and $R_n = 4.6x10^{-5}$ for gold. Normal incidence reflectivity are very small for all material over soft X ray range, which means that conventional mirror used in this way are impracticable.

1.4 Enhancement of Reflectivity

The reflectivities of surfaces for X rays wavelength may be increased by using grazing angle incidence. If, in equation 1.26 and 1.27, the glancing angle is such that

$$(\overline{n}^2 - \cos^2 \vartheta)^{\frac{1}{2}} = 0 \tag{1.30}$$

then the reflectivity is identically equal to unity. For a non absorbing medium ($\beta = 0$), total reflection is obtained for glancing angles smaller than the critical angle ϑ_c, where

$$\cos \vartheta_c = n = 1 - \delta \tag{1.31}$$

For real media, the reflectivity approaches unity as $\vartheta \to 0$. If $\beta << \delta$ a sharp increase in reflectivity is obtained as ϑ fall below ϑ_c; for $\beta \sim \delta$, a more graduate transition occurs. For $\vartheta < \vartheta_c$ no wave can propagate in the mirror material and the incident energy is reflected ("total external reflection"). Calculated grazing incidence reflectivity (for s polarization) are shown for beryllium, carbon, and gold at $\lambda = 3.5nm$ in Figure 1. The p-polarization reflectivity not significantly different. A major problem with grazing incidence optics is their severe aberration, especially astigmatism that can be .

Capitolo 2

Mirrors for X-rays

"Terence: Tu lo reggi il whisky?
Bud: Beh, i primi due galloni si, al terzo divento nostalgico e ci può scappare la
lite... E tu lo reggi?
Terence: Eh, che domande, io sono stato allattato a whisky!"

I due superpiedi quasi piatti

A spherical surface is defined by only one parameter, the radius of curvature of the surface. A spherical surface has the property that the rate of change of the surface slope is exactly the same everywhere on the surface, and thus the aberration is inevitable. This shape bring an intrinsic aberration ("spherical aberration"). If a beam having rays parallel to the optical axis, with a big aperture, hits a concave mirror, as shown in Figure 3, the rays will not focus in the same point "focus", but they converge at the circumference of a circle. So, the image, is not any more a single point but a spot, beams at different position have different focal points. Consider ray AB parallel to the optical axis at a distance d from it

After the reflection of the mirror AB intercept the optical axis at the point F' from the origin O. The relation between F', the radius of the mirror R and the distance d is

$$\frac{f'}{R} = 1 - \frac{1}{2\sqrt{1 - \left(\frac{d}{R}\right)^2}} \tag{2.1}$$

Equation **??** can be obtained by Figure 4. BF' is the reflected ray of the non-paraxial ray AB, F' is the intersection point with the optical axis. Because the law of reflection

$$\alpha = \beta \Rightarrow \alpha = \gamma \tag{2.2}$$

Therefore $F'BC$ is isosceles and $F'D$ is both median and height, thus

$$DC = \frac{R}{2} \tag{2.3}$$

From the right-angle triangle $F'DC$ we obtain

$$\cos\gamma = \frac{R}{2F'C} \Rightarrow F'C = \frac{R}{2\cos\alpha} = \frac{R}{2\sqrt{1-\sin^2\alpha}} \tag{2.4}$$

From the right-angle triangle CGB

$$\sin\alpha = \frac{d}{R} \tag{2.5}$$

The last two equation combined with

$$OF' = OC - F'C \Rightarrow f' = R - F' \tag{2.6}$$

When $\frac{d}{R} \to 0$ then $\frac{f'}{R} = \frac{1}{2}$, therefore

$$f' = \frac{R}{2} \tag{2.7}$$

and the mirror is ideal

If the slope in not any more constant all over the mirror but become flatten in the region surrounding the outer rays, it is possible to focus all the rays in the same point. While correction of spherical aberration is not the only application of aspherical surfaces, it is one of the major application areas. On the contrary from spherical surface, aspherical surfaces cannot be defined with only one curvature, this kind of aspherical surfaces are usually defined by an analytical formula. There exist different kind of aspherical surface with different properties, if there is not the rotational symmetry it is possible to have either a *biconic* surface with two basic curvature and two conic constant in two orthogonal direction or as an *anarmorphicasphere*, which has additional higher-order terms in two orthogonal directions. Another form of aspheric surface is a *toroidal* or *toric*. This shape is a surface of revolution with a hole in the middle, like a doughnut, forming a solid body. This shape is caraterized by two radii, the overall outer radius and the smaller cross-sectional radius. The good point of this geometry is the minimization of astigmatism that make it possible to focus on a small spot, differently form the spherical ones.

2.1 Conic Surfaces

A special kind of aspherical surfaces is those named "*conicsurfaces*" that can be defined as

$$z = \frac{cr^2}{1 + \sqrt{1 - (1+k)c^2r^2}} \tag{2.8}$$

where c is the base curvature at the vertex, k is a conic constant, and r is the radial coordinate of the point on the surface. In Table 2.1 it is shown how the different shape are obtained changing the conic constant k

A good point that have the conical surfaces are the no-presence of spherical aberration. If the object is at the center pf curvature of the surface there are no aberration. Considering an ellipsoid, it is possible to form aberration-free-image for a pair of real image, similar to a hyperboloid mirror. For parabolic mirror there is only one point

Conic Constant k	Surface Type
0	Sphere
$k < -1$	Hyperboloid
$k = -1$	Paraboloid
$-1 < k < -0$	Ellipsoid
$k > 0$	Oblate Ellipsoid

Tabella 2.1: Parameter of different conic surfaces

that make a perfect image of a point for an axial object at infinity. This parabolic behaviour is the main point that make those mirror widely used in astronomical optics. Moving axially the object from the free-aberration point induce a certain amount of spherical aberration: If the movement is laterally, different type of aberration are induced such as: coma, astigmatism.

2.2 Compound Optical system

A further step to obtain a better image is that to use a more than one mirror in order to have o perfect image at the focus. The system that whose invented which respect the sine-Abbe-conidtion are the wolter system that are widely used in astronomy, using combinations of coaxial and confocal conic section.A first approximation system that respect the sine Abbe condition are the Kirkpatrick-Baez system and Montel or nested-Kirkpatrik-Baez system, those compound optical system involves reflector whose meridian planes are at right angle (crossed).

2.2.1 Sine Abbe condition

2.2.2 Wolter System

In 1952 Wolter published a paper in which he discussed several disposition of two conical mirror in order to collect light for an astronoical use. Figure show the different disposition discussed: Wolter I, Wolter II, Wolter III. Wolter I telescope consist of a coaxialparaboloid (primary mirror) and hyperboloid (secondary mirror). The focus of the paraboloid is coincident with the rear focus of the hyperboloid, and the reflection inside both mirrors. The Wolter II telescope use the same kind of mirror of Wolter I paraboloid and hyperboloid. But the focus of the paraboloid coincident with the front focus of the hyperboloid, and, the reflection, occurs internally for the paraboloid and externally for the hyperboloid. The Wolter III telescope consist in a paraboloid and an ellipse. In this system the first mirror is the paraboloid one, and the second is the ellipsoidal that have front focus coincident with that of the parabola, moreover the reflection is external for the paraboloid and internal for the ellipsoidal. The Wolter I have typical grazing angle of less than a degree and is used for hard X-rays. The Wolter II telescope has typical grazing angle of, approximate, 10 degree and is used for soft X rays and extreme ultraviolet (EUV). Because of circular symmetry, astigmatism and spherical aberration are eliminated

but exhibit coma aberration. Other problem is the difficulty of fabrication , and require a huge area to achieve a very small collecting angle.

2.2.3   Kirkpatrick-Baez System

This kind of optics are used in the ESRF and consist, as shown in Figure, in two separated cylindrical surface conical mirror that focus the incident beam in both saggital and transverse thus astigmatism is removed. Although such system introduce another type of distortion, anamorphotism. Because of the different distance of the image plane with respect to the mirrors the magnification is different in the two direction. Another technical problem that face with system is the big volume that occurs to implement it. To overcome those two problem and obtain a system that conjugate the good behaviour of the KB system with an equal magnification of the two direction and compact system, it is possible to implement a system as it is showed in Figure, a system in which both mirrors are at the same distance from the object. This sort of arrangement is extremely difficult to manufacture and, consequently, very expensive. Despite these problem K-B system are very used in ESRF and in European synchrotron, on the contrary, in American synchrotron another type of optical system, named "Montel", is used that will be discussed in the next section.

2.3   Montel

As discussed before KB system have some limitation that can be overcome with a different optical system named "Montel". This geometry bring four important advantages for high-precision focusing:
i) the optical system is more compact which allow greater working space;
ii) the focal distance of the two mirror are the same, this cancel out the anamorphotism;
iii) the alineation of the system is easier with respect to the KB system because, in this case, only one thing has to be aligned, on the contrary, in the KB there are two separated mirror that has to be aligned;
iv) the divergence that can be collected is larger which allows for greater flux and/or a lower diffraction limit.

2.3.1   Optical Design

The mirrors used in this Montel configuration are mirror that have a cylindrical shape in one direction and elliptical shape in the other direction. One approach to obtain the Montel system is that to use two pre-figured elliptical mirror and grind the cut site at 45° as shown in figure. After that it place the mirrors together makes a good fit with no gap requiring no contouring of the mirror side. Another way involves diveding pre-figured elliptical mirror into two part that, add them together, can form the Montel system. This approaches is primary driven by the fact that in a conventionally polished mirror, the clear aperture area has the best figure and finish. As such uAs such, using two halves of a prefigured mirror cut in the

middle has several advantages- including consistency and economy. There are major challenges however. First, the mirror surface must be protected against damage and deformation during cutting and subsequent figuring operations. After cutting into two, the cut sites must be treated (e.g., etched) to remove any subsurface damages that could alter a mirror's figure. Then the mating side of one of the mirrors must be contoured and polished such that when it is placed against the partner mirror, it makes a nearly perfect fit with good surface quality all the way to the contact edge.This last two-steps are crucial because if there is a significant gap or if the mirror surfaces in the vicinity of the interface are damaged, a significant part of the incident beam could be lost. As an example, we are developing a pair of Montel mirrors for polychromatic nanofocusing on Sector 33 at APS. This beam line will use 40 mm long elliptical mirrors for nano-focusing a 100 μm beam to a 50 nm spot at 2000x demagnification. This concave elliptical mirror has a maximum depression of about 6 μm at its center. If cut flat and placed against its mating mirror, a gap as large as 6 μm is created which loses about 10% of the 100 μm incident beam. Similarly, if the mirror surfaces near the intersection are damaged, then beam loss can be significant.

Capitolo 3

MONWES

"Bud: No, calma, calma, stiamo calmi, noi siamo su un'isola deserta, e per il momento non t'ammazzo perché mi potresti servire come cibo ..."

Chi trova un amico trova un tesoro

My thesis' work is the creation of a python script that simulate a ray-tracing of a beam. This tracing take in account the effect of different type of optical elements that that can find the beam in its way. To implement this ray-tracing it have to define three elements:
- Beam
- Optical elements
- Tracing system

3.1   Beam

Beam object is the object that contain the spatial and velocity information of a collection of rays. The Beam object is mainly charecterized by four parameters:

- Number of rays

- Spatial profile

- Divergence profile

- Flag vector

Starting from the begging it can say that having a large number of rays is useful in terms of results but, as a back draw, increase the computation time, so, it have to find a compromise between the number of rays and the computation time depending on the quality desired. By default, the number of rays, is setted $25*10^3$ that allow to have good results without spending lot of time. To change the number of rays it need to do as in figure 3.1, where, the number of rays is choose as 10^4.

```
1    from monwes.Beam import Beam
2
3    beam = Beam(N=10**4)
```

**Figura 3.1:** Example of Beam definition

Defined the Beam with its number of rays it have to choose the spatial and divergence profile. For the spatial profile there are some possibilities that correspond to different geometrical figure such as: rectangular profile, circular profile, Gaussian profile, point wise profile. The default one is the point wise profile, that it is useful for ideal testing, obviously, for this case,there is no input parameter. All the other profile are characterized by external input in order to define the profile depending on the nature of the profile. for the Gaussian profile the parameter needed is the σ_x and σ_z that correspond the the σ of the two dimension, Figure 3.2a show a code example to define a Gaussian spot of a Beam having $25 * 10^3$rays with the two σ different, $\sigma_x = 0.1mrad, \sigma_z = 1mrad$ as it is showed in Figure 3.2b.

```
1    from monwes.Beam import Beam
2
3    beam = Beam()
4    beam.set_gaussian_spot(1e-4, 1e-3)
```


(a) Example code for a Gaussian spot
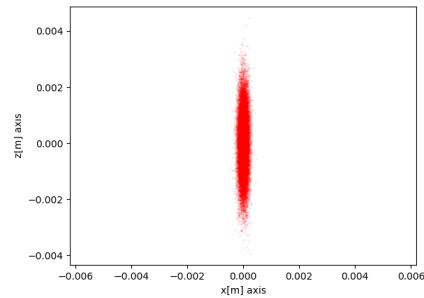
(b) Plot of Figure 3.2a

Figura 3.2: Example 1

Over the Gaussian profile, there are other two geometrical profile that can be defined rectangular and circular that have a uniform distribution, of the rays, in their space domain. For the rectangular distribution the parameter to define are the xz limit of the coordinate that define the sides of the rectangle. Figure 3.3a show an example code where it is defined a circular profile with a radius of 1cm and, after, overwritten another geometrical profile having a rectangular shape, in this case the final profile of the Beam is that figured out in Figure 3.3b, a rectangular non symmetric profile with the coordinate defined in the code in Figure 3.3a.
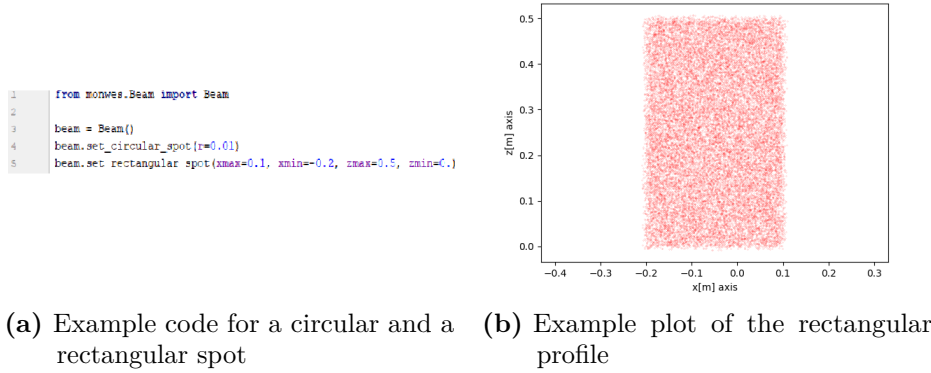
```
1    from monwes.Beam import Beam
2
3    beam = Beam()
4    beam.set_circular_spot(r=0.01)
5    beam.set_rectangular_spot(xmax=0.1, xmin=-0.2, zmax=0.5, zmin=C.)
```

(a) Example code for a circular and a rectangular spot

(b) Example plot of the rectangular profile

Figura 3.3: Example 2

Moreover it is possible to define a special shape that have, more or less, the figure of a person with a uniform distribution of the point in all the point of the space. This special shape is showed in Figure 3.4a, that is defined in the code written in Figure 3.4b. As it is showed, the initialize_ as_ person command take two input parameter, the number of the total rays (by default are $25 * 10^3$), and a size parameter that set the coordinate limit of the figure, more precisely. In Figure 3.4a the size correspond to 10^{-6} so the limit are:

- $x_{max} = 1\mu m$

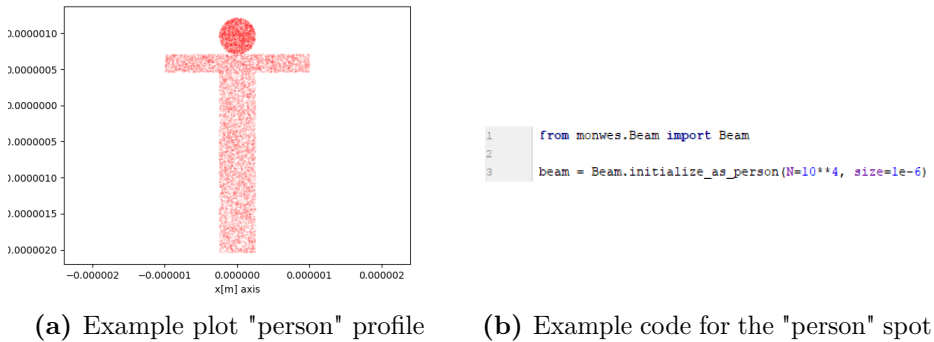- $x_{min} = -1\mu m$

- $z_{max} = 1\mu m$

- $z_{min} = -20\mu m$


```
1    from monwes.Beam import Beam
2
3    beam = Beam.initialize_as_person(N=10**4, size=1e-6)
```

(a) Example plot "person" profile

(b) Example code for the "person" spot

Figura 3.4: Example 3

The last piece of the Beam object is the "Flag" vector. Every component of this vector have a correspondence with a certain ray and contain the information about the number of optical element that, the ray, travel until a particular moment. Moreover this value become negative when the ray doesn't hit an optical element,

in such a way to have an information where the rays were lost. Figure 3.5, resume the main parameter of the Beam object with their default values

```python
8     class Beam(object):
9
10        def __init__(self,N=25000):
11
12            N = round(N)
13
14            self.x = np.zeros(N)
15            self.y = np.zeros(N)
16            self.z = np.zeros(N)
17
18            self.vx = np.ones(N) * 0.
19            self.vy = np.ones(N) * 1.
20            self.vz = np.ones(N) * 1.
21
22            self.flag = np.zeros(N)
23
24            self.N = N
```

Figura 3.5: Resume of the Beam object parameter

A part from the principal characteristic treated above, Beam object contain other option in order to manage better the utilization of it. The other option defined are reported here below:

- import_ from_ file(filename='filename'): define a Beam with a characteristic defined in a file '.h5'

- set_ point(x,y,z): move the Beam in a part of the space centred in the coordinate (x,y,z)

- initialize_ from_ arrays(x, y, z, vx, vy, vz, flag): define a Beam with the spatial value defined in the array x,y,z, the velocities' value defined in the array vx,vy,vz and the flag value defined in the array flag

- duplicate(): duplicate a Beam

- good_ beam(): define a Beam that, starting from another Beam, extract only the good rays (those that have a positive flag)

- part_ of_ beam(indices): define a Beam that, starting from another Beam, extract the ray that correspond to the position defined in the array indices

- number_ of_ good_ rays(): return the values of the good rays

- merge(beam2): merge a beam1 with another beam2, the first part of this new beam correspond to the beam1, and the second part to the beam2

- retrace(distance): this correspond to a free propagation in the space of the Beam within a distance equal to "distance"

At the end there are the command that plot the various characteristic of the beam, that contain the information for the plotted characteristic, for example plot_ xy() make a plot of the x and y coordinate of the beam, plot_ good_ xpzp() make a plot of the x-velocities and z-velocities of only the rays that have a positive flag

3.2 Optical Elements

Because, as discussed in Chapter 1, mirrors are the principal elements used in synchrotron the main optical element developed is the mirror, but it is also defined an ideal lens that is useful to simulate some particular profile for the Beam.that corresponding to this , more attention is focused on them, on the contrary , for testing uses, only one kind of lens, an ideal lens, is implemented.

3.2.1 Mirrors and lens

The different kind of mirror that are defined are:

- plane mirror

- sphere mirror

- ellipsoidal mirror

- paraboloidal mirror

- hyperboloidal mirror

All those geometrical shape are a subset of a surface conical figure. As is discussed in Chapter 2, and reported in Equation 3.1, a surface conic is defined by a series of coefficient.

$$a_0 x^2 + a_1 y^2 + a_2 z^2 + a_3 xy + a_4 yz + a_5 xz + a_6 x + a_7 y + a_8 z + a_9 = 0 \quad (3.1)$$

The parameter needed to define the correct surface conic shape that define uniquely the mirror desired are:

- focal distances

- angle of incidence ϑ_g, more precisely the program use the complementary angle of ϑ_g that is $\vartheta = \frac{\pi}{2} - \vartheta_g$ (the input and output angle are in radiant)

Moreover, the surface conic, is defined in such a way to have the origin equal to the incidence point of a collimated ray distant p (that correspond to the object focal distance) from the mirror, and with the normal of the surface corresponding to the z-axis, as it is showed in Figure 3.8. For the plane mirror the situation is simple, because the equation of the surface is that in Equation 3.2, that have all the coefficient equal to 0 apart from a_8 that is equal to 1.

$$z = 0 \quad (3.2)$$

For the spherical case, the parameter that characterize a sphere is the radius, one time defined the radius, the equation of the sphere is:

$$x^2 + y^2 + z^2 = r^2 \quad (3.3)$$

Moreover, it is known, from the spherical lens optics, that

$$\frac{1}{p} + \frac{1}{q} = \frac{2}{r_t \sin \vartheta_g} \tag{3.4}$$

and

$$\frac{1}{p} + \frac{1}{q} = \frac{2 \sin \vartheta_g}{r_s} \tag{3.5}$$

where r_t, is the tangential radius, and r_s is the saggital radius. The sphere case have $r_t = r_s$, this mean that, apart from the normal incidence case, the sphere cannot perfectly focolize/collimate a beam. The radius choosen in Surface_ conic object is that corresponding to the equation 3.4:

$$r = \frac{2}{\cos \vartheta} \frac{pq}{p+q} \tag{3.6}$$

where p correspond to the object focus length, q to the image lengths, ϑ_g to the incidence angle and $\vartheta = \frac{\pi}{2} - \vartheta_g$.

For the paraboloid shape, to find the correct coefficients that define the right surface, it is needed the incidence angle, one focal distance and another parameter that distinguish between the two behaviour of the mirror that are showed in Figure 3.6a and, Figure 3.6b. This two system correspond mirrors that, physically, have different behaviour, the first one Figure 3.6a, focalize a Beam, the second one, Figure 3.6b, collimate a Beam.
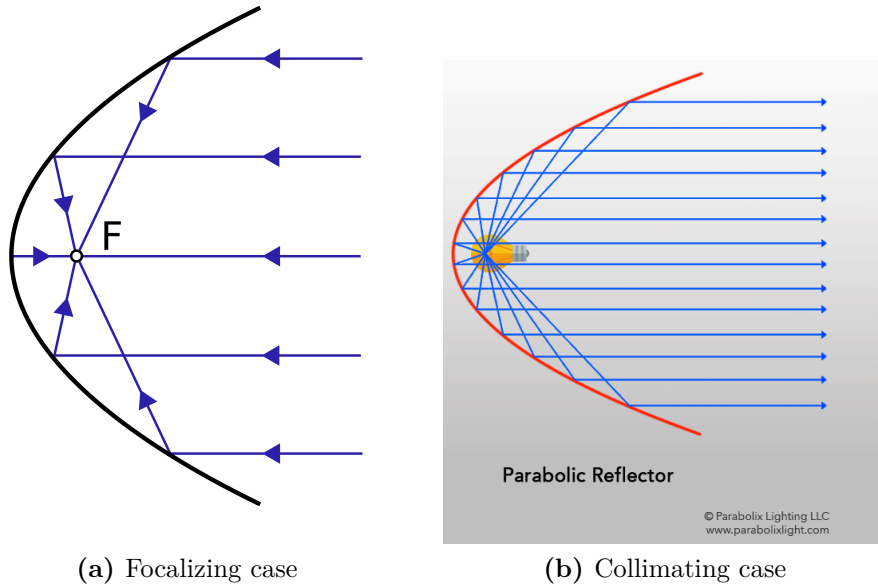

(a) Focalizing case   (b) Collimating case

Figura 3.6: Parabola

The general equation of a parabola, such that in Figure 3.7 is

$$y = \frac{1}{4f} x^2 \tag{3.7}$$

where f is the focal distance of the parabola. After a few calculation, see Appendix A, it is possible to correlate f with the input parameter in this sense

$$f = d \sin^2 \vartheta \tag{3.8}$$

where d is the object focal distance, in the case depicted in Figure 3.6a, otherwise, in the case depicted in Figure 3.6b, d is the image focal distance.
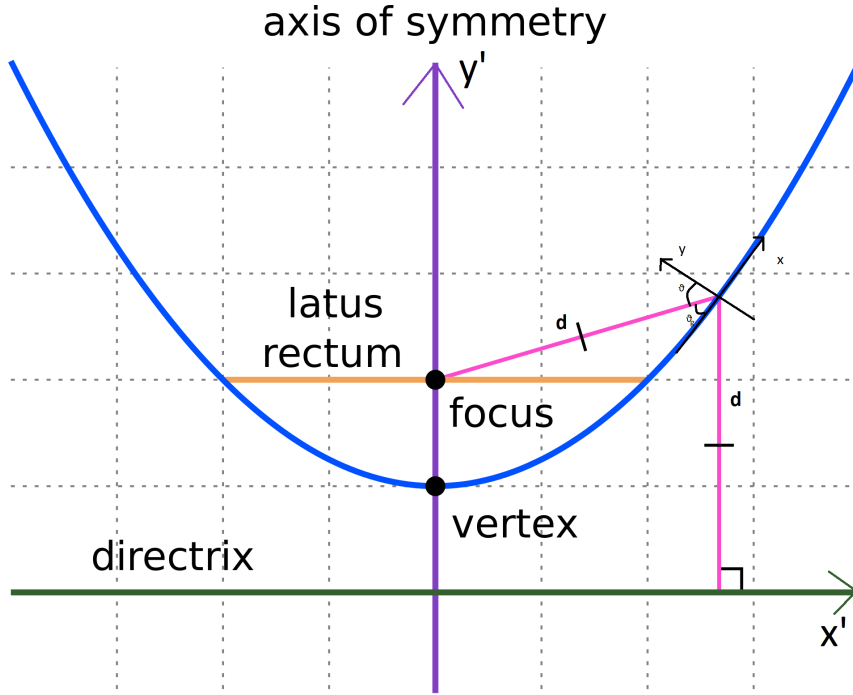

Figura 3.7: System

For the elliptical case the situation is rappresented in Figure 3.8. Equation 3.9 describe the general equation of an ellipse where appear two unknown a and b.

$$\frac{x^2}{a^2} + \frac{y^2}{b^2} = 1 \tag{3.9}$$

It is possible to correlate (Appendix A), the focal distances plus the incidence angle with the two parameter a and b with the following two equations:

$$p = \frac{a+b}{2} \tag{3.10}$$

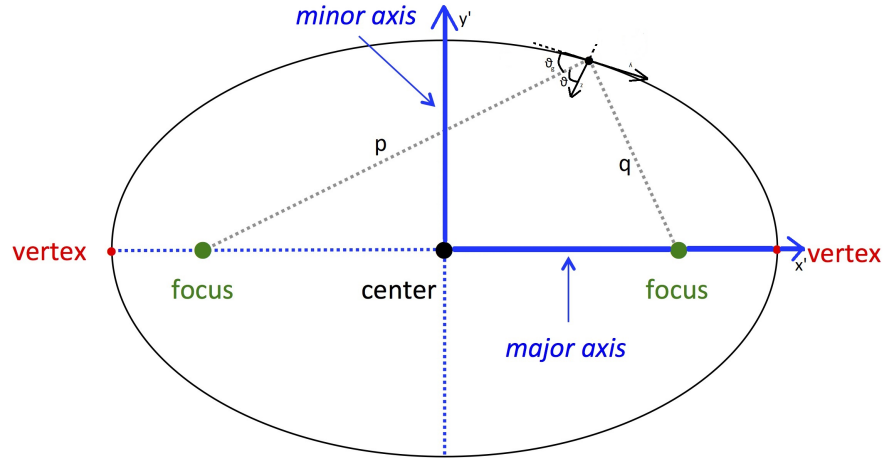$$q = \sqrt{ab} \sin \vartheta \tag{3.11}$$

Figura 3.8: Ellipse System

Defined the surface in the $x'y'$, it is done a rotation and a translation in order to center the new xy system on the point P with the normal at that point equal to the z-axis.

For the hyperboloidal mirror the situation is similar to that of the ellipsoidal case, in fact, the general equation of the an hyperbola such the one in Figure is

$$\frac{x^2}{a^2} - \frac{y^2}{b^2} = 1 \tag{3.12}$$

and the equations that correlate the focal distances and the incidence angle with the parameter a and b are

$$p = \frac{a - b}{2} \tag{3.13}$$

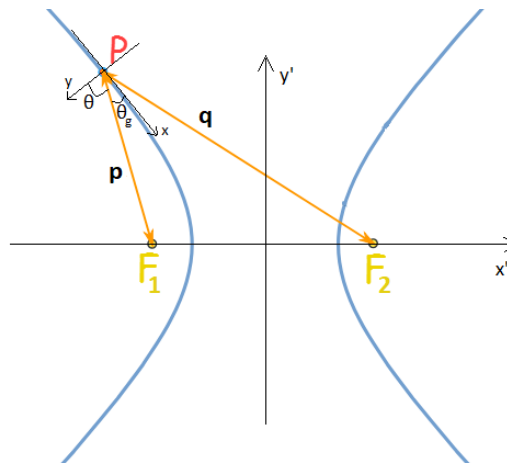$$q = \sqrt{ab}\cos\vartheta \tag{3.14}$$

Figura 3.9: Hyperbola System

After that it, as in the case of the ellipsoidal mirror, it need a rotation and a translation to complete the work. For the mirrors, in the program, there is a further

option that make the mirror cylindrical in one dimension maintain its surface conic in the other, to do this, in Surface_ conic object, it is defined a function set_ cylindrical, that change the shape of the surface, from a complete surface conic, to a surface conic in one dimension and cylindrical in the other.

Apart of the mirrors elements is implement also an ideal lens element that follow the typical lens equation:

$$\frac{1}{f_x} = \frac{1}{p} + \frac{1}{q} \tag{3.15}$$

$$\frac{1}{f_z} = \frac{1}{p} + \frac{1}{q} \tag{3.16}$$

where f_x is the x focal length and f_z is the z focal length. For this optical element the input parameters are the object focal distance, image object distance and the two focal distances (f_x, f_z) that, in the default mode, are setted equal with a value equal to $f_x = f_z = \frac{pq}{p+q}$.

3.2.2 Compound Optical Element (KB and Montel system)

This program include also two different system composed by more mirrors. Starting from conical mirrors, combining them, is possible to have a compound optical elements that can simulate the behaviour of some typical instrumentation that characterize the facilities, in particular in the synchrotron world. The compound optical system implemented are two of those mentioned in Chapter 2:

- KirkPatrickBaez system (KB system)

- Montel

KirkPatrickBaez or, more simply, KB system are shown in Figure 3.10 is composed by two cylindrical surfacing conic mirror placed one after the other with the two focal lens that converge in the same point. There are implemented two different kind of KB system, a first one composed by two elliptical mirrors and a second one composed by parabolic mirrors. The input parameter that the program need are the two incidence angle and the two focal, with respect to the center of the KB system, represented in Figure 3.11 and the separation of the two mirror, from center to center.
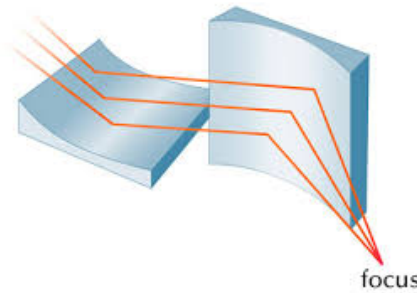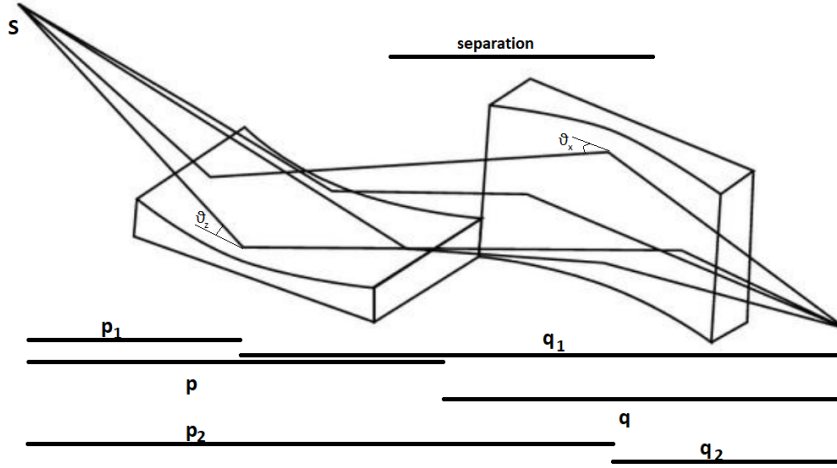

Figura 3.10: System

Figura 3.11: System

Because this system is simply a system composed by two surface conical mirror in series the parameter that the system need to define the mirror are not the ones defined by the user but are the focal distance of the two mirrors that are, as shown in Figure, p1, q1, p2, q2, These parameter represent the object focal distance (p1, p2) and the image focal distances (q1, q2) of the two mirror, as represented in Figure 3.11. Figure 3.12, show an example of the definition for a KB system that have an object focal length of 2m, an image focal distance of 5m, a separation between the two center of the mirrors of 1m, and the two angle of incidence equal each other to 2°.

```
1  from monwes.CompoundOpticalElement import CompoundOpticalElement
2  import numpy as np
3
4  theta = 88. * np.pi / 180
5  KB = CompoundOpticalElement.initialize_as_kirkpatrick_baez(p=2., q=5., separation=1., theta_z= theta)
```

Figura 3.12: Example 5

The Montel system, depicted in Figure 3.13, is composed, as for the KB, by two surface conical mirror cylindrical in one direction, but, because the two mirror are not in series, as for the case of the KB, the situation is a bit complicate. Starting from definition of the two mirrors one is rotated of 90°, in order to have a mirror in the xy plane, and another one in the zy plane. As shown in Figure 3.13 the center of the Cartesian system is setted in the point where the optical axis of the system hit the compound system having the normal of the first normal equal to the z-axis, and the second normal equal to the - x-axis. The system is defined by the following parameter p, q, ϑ_z, ϑ_x, where p and q are the focal distance of the two mirrors and ϑ_z and ϑ_x are the angle of incidence to define the correct mirrors (by default $\vartheta_z = \vartheta_x$).
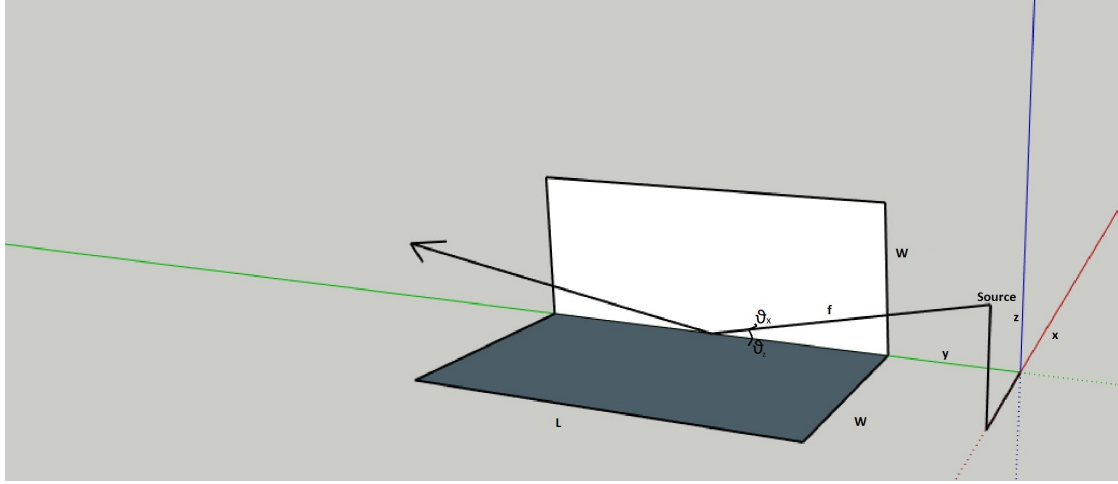
Figura 3.13: System

The following Figure 3.14 show an example code for a parabolic Montel system having an object focal length of 5m, image focal length of 2m and the two incidence angle of 1.5°, that focalize a Beam. As for the KB system also in this case there are implemented two possibilities, an ellipsoidal system (having the two mirror as ellipsoid), and parabolic system (having the two mirror as ellipsoid).

```
1    from monwes.CompoundOpticalElement import CompoundOpticalElement
2    import numpy as np
3
4    theta = 88.5 * np.pi / 180
5    montel = CompoundOpticalElement.initialize_as_montel_parabolic(p=5., q=2., theta_z=theta, infinity_location='p')
```

Figura 3.14: Example 6

3.3 Tracing System

Defined the Beam and the different optical element, to complete a simulation, is needed a tool that put everything together and modify the property of the beam after the interaction with the optical elements.

For example, if it want to simulate the system depicted in Figure 3.15, it have to define a Beam source, the optical element and, at the end, somewhere, the distances between the optical elements. The tracing part of the program, for the non-compound optical element, is written in such a way that the trace work in series, one optical element after the other. This, in series methods, work with the definition of two distances, object/image distance from the center of the optical element, the incidence angle of the Beam, that can be different from the designing one, and a second angle that define the mirror with respect to the Beam. (normally and also for the default case the incidence angle i equal to the designed one, and the second angle is fixed to 0°). One possibilities, to define the systam in Figure 3.15 is to set the object distances of the mirrors equal to distance d_0 and d_1, and the image distances equal to 0, for the lens lets set the object distance equal to d_3 and the image distance equal to d_4 as it is reported in Figure 3.16.
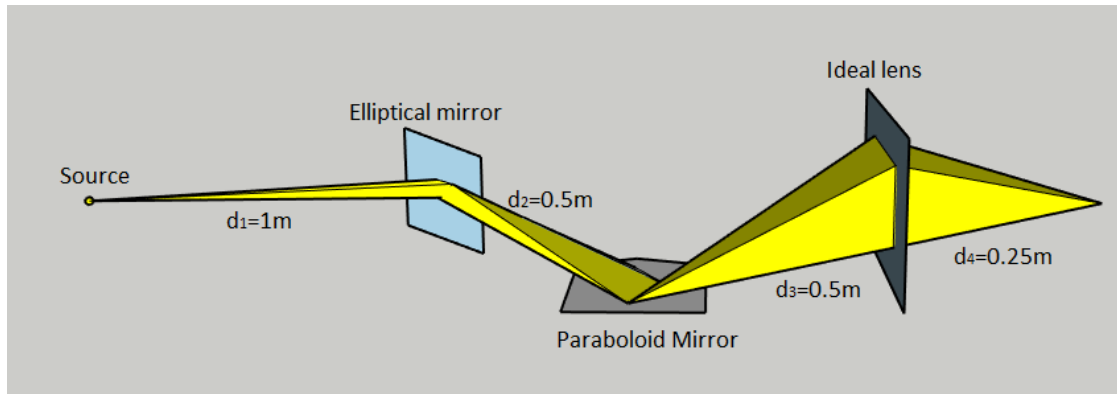
Figura 3.15: System

```
1    import ...
5
6
7    theta_e = 88.5 * np.pi / 180
8    theta_p = 88. * np.pi / 180
9    beam = Beam()
10   beam.set_gaussian_divergence(1e-3, 1e-4)
11
12   ell = Optical_element.initialize_as_surface_conic_ellipsoid_from_focal_distances(p=1., q=2., theta=theta_e)
13   par = Optical_element.initialize_as_surface_conic_paraboloid_from_focal_distances(p=0.5, q=2., theta=theta_p, infinity_location='p')
14   lens = Optical_element.initialiaze_as_ideal_lens(p=1., q=2.)
15
16   beam = ell.trace_optical_element(beam, p=1., q=0)
17   beam = par.trace_optical_element(beam, p=0.5, q=0., alpha=np.pi/180)
18   beam = lens.trace_optical_element(beam,p=0.5, q=0.25)
```

Figura 3.16: Example 7

3.3.1   Tracing for simple Optical element

Going deeper in the code, the algorithm that trace a single element is divided in 5 step

1. change the reference system with that soldal with the optical element after two rotation, one along x-axis, and second along y-axis, and a translation equal to the object distance of the optical element

2. free propagation up to the optical element

3. effect of the optical element

4. free propagation to the image plane

5. changing the Cartesian system in that one that have the optical axis equal to the y-axis

The first three point are condensed in the method effect_ of_ the_ optical_ element, that is showed in Figure 3.17a, and the last two point are condensed in the method effect_ of_ the_ screen that is showed in Figure 3.17b.

(a) Example code for a Gaussian spot

(b) Plot of Figure 3.2a

Figura 3.17: Example 1

Because of the different definition, the tracing method of the rays' beam, need a different interpreter that can link the beam with the different optical elements that meet on his way. Because of the different nature, there are implemented two kind of tracing, a first one that trace the KB system, that is composed by a series of optical elements and so can be used for all the compound optical elements that are in series. And a second one that is specific for the Montel system, because it is not composed by mirrors in series rather than mirrors in parallel, having the two elements in a very small region of the space that have in which order the rays of the beam hit the different mirrors.

3.3.2 Tracing for KB

For KB system the situation is more or less the same as for a simple optical mirrors, with the only difference that there are more than one mirror. So the algorithm to simulate the tracing system is nothing else than a for loop, that use the tracing system of the simple optical element. In this the object and the image distance from the center of the system are the default ones, such as for the incidence angles. Figure 3.18, show the trace code for the compound elements that are in series.
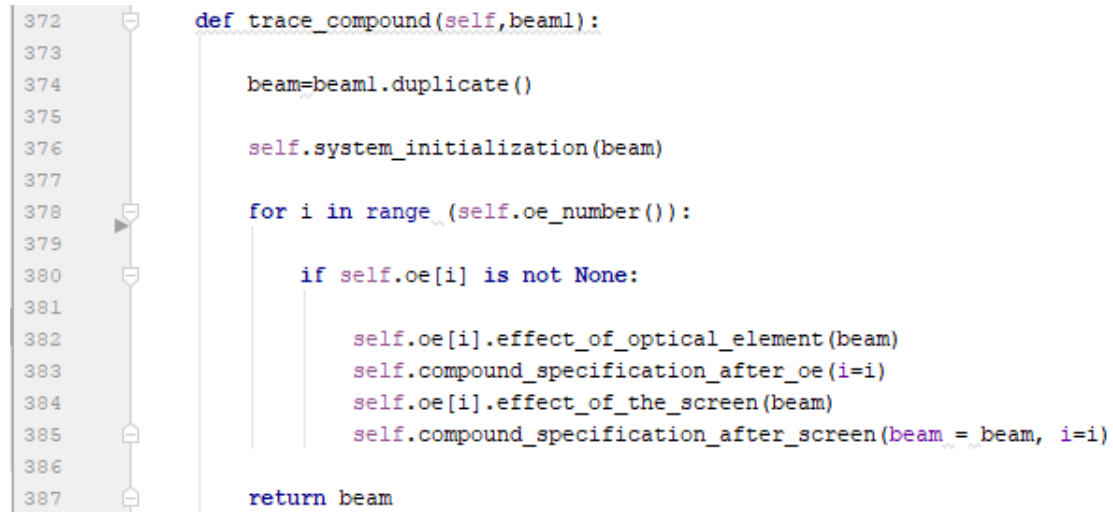
```
372    def trace_compound(self,beam1):
373
374        beam=beam1.duplicate()
375
376        self.system_initialization(beam)
377
378        for i in range (self.oe_number()):
379
380            if self.oe[i] is not None:
381
382                self.oe[i].effect_of_optical_element(beam)
383                self.compound_specification_after_oe(i=i)
384                self.oe[i].effect_of_the_screen(beam)
385                self.compound_specification_after_screen(beam = beam, i=i)
386
387        return beam
```

Figura 3.18: Example 8

3.3.3 Tracing for Montel

Montel system is completely different from the KB system and all the series optical system, so it need a new trace system. This new trace system is divided as

follow

1. Changing the reference frame in one having the center on the center of the mirrors, with a z-axis corresponding to the normal of one mirror and -x-axis equal to the normal of the second mirror. This transformation is done in a similar way of the normal tracing, two rotation of the beam, and one translation, differently from the normal tracing, the tw rotation are done such that the beam hit the mirrors with an incidence angle set by the user

2. Focus the attention on the travel time of each ray in order to know which is the nearest optical element of each ray

3. free propagation of each ray up to the nearest optical element

4. effect of the system for each ray

5. repeat the 2nd, 3rd and 4th passage two times, in order to consider the two reflection

6. Change the reference system solidale with the beam that is subject to two reflection, doing two rotation and one translation

What is reported above is the default tracing system that, because of its centrality on my thesis' work have many option. What is setted by the user is

1. focal distances and incidence angles, that define the two rotation and the translation of the tracing system

2. name of the File in which is saved the data of the simulation, by default no data is saved

3. there is the possibility to choose a different point, from the origin, in which the the optical axis hit the system

4. there is also the possibility to have a final output frame that is not solidal by the two-reflected beam, but with the non reflected beam or with the other two beam that are reflected only one time

5. It is also the possibility to figure out the footprint of the two reflected beam on the system. For clarity the beam that hit the first mirror and after the second is labelled with red point, the beam that hit the second and after first mirror is labelled by blue color

These options are added in order to study better the behaviour of a beam with a Montel system. The possibilities to change the angle of incidence and to hit different part from the origin can be used to study what happen to a beam when is not aligned, or not perfectly aligned, and use these result to align the system in the laboratories. The possibilities to save a File is useful in particular in those case where there is a huge computational effort that need a lot of time, in these cases is possible to work with the result of a big simulation without reappointing it, and so

save time. Figure 3.19 show the code that trace a Montel elements, containing also the special option that were defined above.

```python
def trace_montel(self, beam, name_file=None, mode=0, p=None, q=None, theta_z=None, theta_x=None, hitting_point=Vector(0., 0., 0.),
                 output_frame=0., print_footprint=1):

    self.oe[0].set_parameters(p=p, q=q, theta=theta_z)
    self.oe[1].set_parameters(p=p, q=q, theta=theta_x)

    v_in = self.get_optical_axis_in(mode)

    self.input_frame(beam, v_in, mode, hitting_point)


    beam1, beam2, beam3 = self.apply_specular_reflections(beam, name_file, print_footprint)

    if output_frame == 0:
        v_out = self.get_optical_axis_out(mode)
    elif output_frame == 1:
        v_out = v_in

    self.output_frame(beam3[0], v_out, mode)
    self.output_frame(beam3[1], v_out, mode)
    self.output_frame(beam3[2], v_out, mode)



    return beam1, beam2, beam3
```

Figura 3.19: Example 8

Capitolo 4

Results

"Terence: Ma scusa di che ti preoccupi, i piedipiatti hanno altro a cui pensare, in questo momento stanno cercando due cadaveri scomparsi
Bud: Se non spegni quella sirena uno di quei due cadaveri scomparsi lo trovano di sicuro!"

Nati con la camicia

4.1 Testing

To demonstrate the correct behaviour of the program there are done a comparison with respect to the OASYS software for ray tracing simulation, developed by Manuel Sanchez Del Rio, and with respect to the paper [RKM15]. The comparison with OASYS check the correct working of all the component apart from Montel system (mirrors, lens, KB ...), on the contrary, the paper is dedicate for the Montel simulation, because this particular kind of optical system, is not implemented on OASYS.

4.1.1 Testing with OASYS

4.1.2 Testing with the paper

In Figure 4.1 is depicted the Montel system used in the simulation done by the paper in its system of reference. The aim of this system is to collimate a Beam using a Montel with two parabolic mirrors. The source used have a Gaussian dimension with a FWHM of 2.5μm and a Gaussian divergence of $5mrad$. The distances, between the source/image plane and the center of the Montel are, respectively, $\simeq 0.26$m and 10.06m, moreover, the incidence angle of the Beam is $\vartheta_g \simeq 2.86°$. The result, at the image plane, of the beam size and beam divergence, after the double-reflection of the Montel system, is showed in Figure 4.2. Where, in Figure 4.2a, is showed the figure of the beam at the image plane, and, in Figure 4.2c, is showed the divergence. The quantitative values reported on the paper correspond to a Gaussian-like distribution with a spacial FWHM of $\sim$0.7mm, for the spot size, and a FWHM of the Gaussian divergence $\sim$ 0.01 mrad.
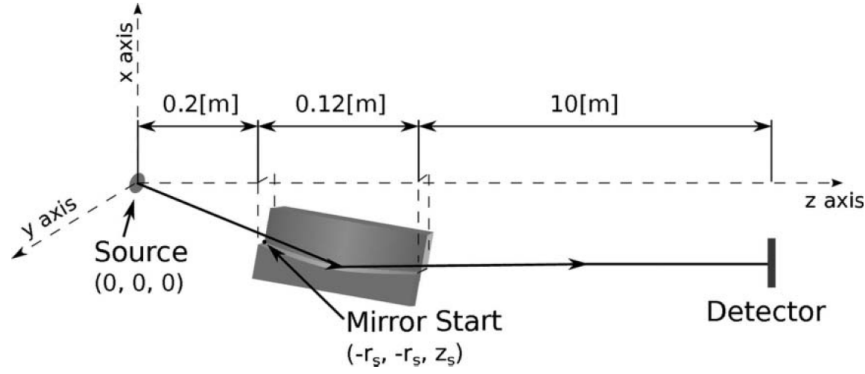
Figura 4.1: Illustration of the Montel system used as a collimator in the paper [RKM15]

Repeating the simulation with my program using the parameter defined in in the paper [RKM15], are figured out in Figure 4.2. As it is showed in the Figure 4.2 there are a qualitative good agreement with the two simulation .Also, under a quantitative point of view, there is a good agreement in fact, in my simulation are obtained a value of ∼1mm of FWHM of image size, pretty similar to the one of the other simulation, and ∼0.01 mrad FWHM of divergence that is equal to the one obtained with the other simulation.

4.2 Analysis of Montel system

In this section it is done, using the Montel tools devolopped, a study of the Montel effect with respect to a Beam, simulating different situation. The first point, to understand that Montel work well, it is simulated the behaviour of a pointwise source with a certain divergence, using a collimating system, and watching what happen to the beam. The second step is to simulate a collimating beam with a certain source shape geometry and figure out the image plot obtained by a focalizing system in its image plane. What is expected is a point, in the velocity space for the first situation and in the real space for the second simulation, because this is the behaviour of an ideal collimating/focalizing system. For the simulation are used parabolical Montel and an incidence angle of 2° (the choice of the angle is arbitrary, that of the paraboic system is because is needed to collimate a beam, also for elliptical system is possible to tcollimate a beam using one focal distance very big).
In Figure 4.3 are reported the result for the ideal collimating/focalizing cases. For the collimation system is used a point wise source with a Gaussian divergence of FWHM of 25μm, 4.3a, to the image plane. As it is showed there is a collimation, but not perfect, this effect is one limit of the Montel because the perpendicular geometry is not the ideal one. Moreover, for the focalizing system, it is used a circular source spot having a radius of 1mm, 4.3c, with a collimated beam, that show, at the image plane 4.3d, a similar behaviour as for the collimation case, for the same reason. Another interested point to show is the footprint on the two mirror that are represented in Figure 4.4. It is possible to note that the area hitted by the beam have a greater component on the y direction (due to the grazing
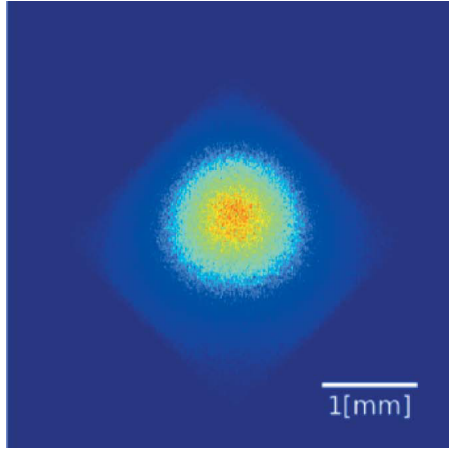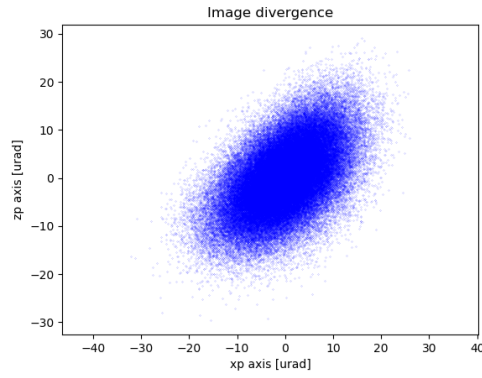
(a) Beam image shape of the paper
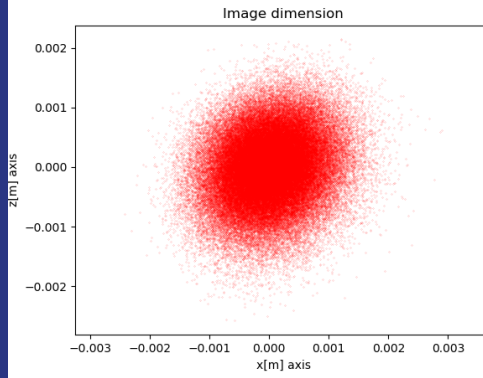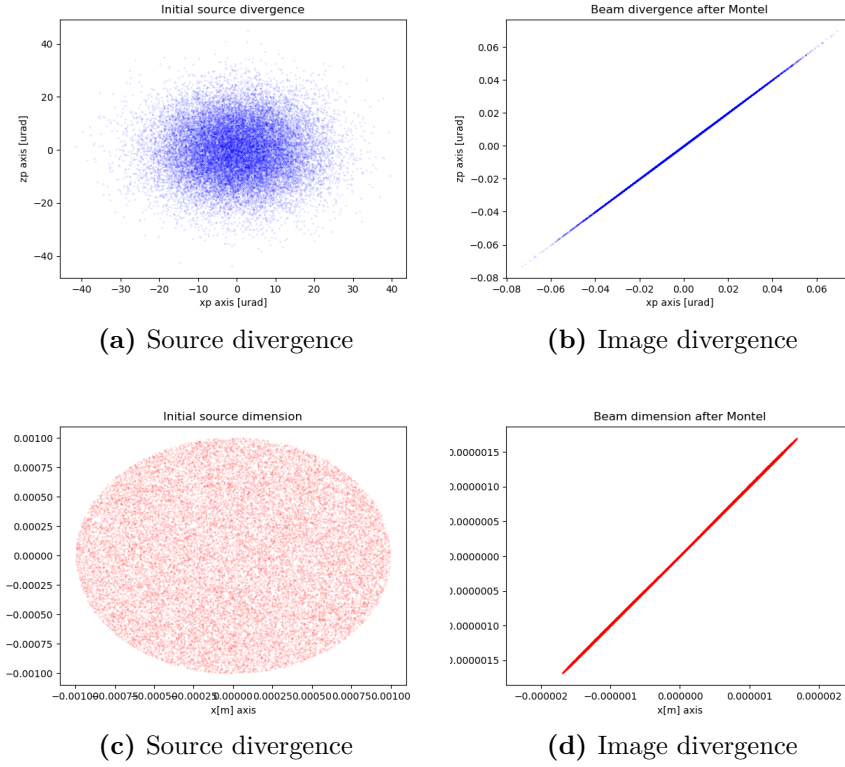
(b) Beam image shape of the simulation
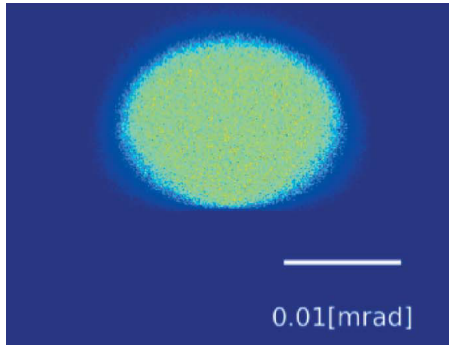
(c) Beam image divergence of the paper **(d)** Beam image divergence of the simulation

Figura 4.2: Results of the Montel simulations with a source beam with a FWHM spot of 2.5μm and a Gaussian divergence of $5mrad$

(a) Source divergence

(b) Image divergence

(c) Source divergence

(d) Image divergence

Figura 4.3: Ideal system

incidence), than in the other direction. In this particular case the x-lenght of the xy-mirror, and the z-lenght of the zy-mirror, is very small (at the order of 20μm) with respect to the y-lenght that is $\sim$20mm. These calculatione are done for a very small Gaussian spot with a FWHM of 1μm and a narrow divergence of FWHM equal to 25μrad. Up to know the dimension of the Montel were not considered, the Montel is setted to have infinite dimension in all the direction. This approach hold in the case of a small source and a narrow profile divergence, otherwise, for example of an isotropic souce that can be modelled with a very big divergence the situation change. In this section, it is used a Beam source with a square shape with a side of 1mm, with a Gaussian profile divergence of FWHM=1mrad in order to show what happen to the Montel where it is covered over all its surface. The focalizing parabolic Montel parameter are:

- object distance: 1m

- image distance: 3m

- incidence angle: 2°

- length of the Monte: 0.1m

- width of the Montel: 20cm

Figure 4.5, show thee image plane of the Montel defined above. This plot show 4 figure, the biggest one, reppresented by the red dots, correspond to the rays
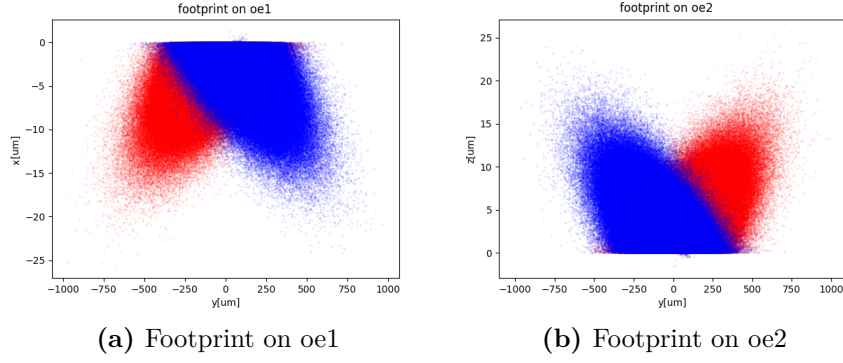
(a) Footprint on oe1

(b) Footprint on oe2

Figura 4.4: Footprint, on the xy-mirror (4.8a) and on zy-mirror (4.8b). The red dots are those rays that hit before xy-mirror and after zy-mirror, the blue ones hit first xy-mirror and after zy-mirror.
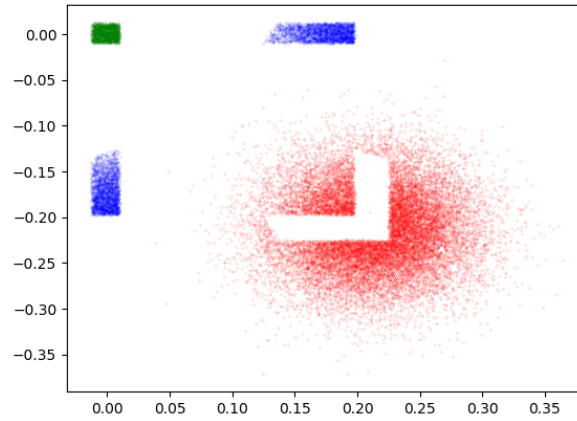

Figura 4.5: Illumination at the image plane of the different Beam (red dots correspond to np-reflected rays, blue dot to one-reflected rays, green dots to two-reflected rays).

that reach the image plane without touch the Montel, the rays coloured in blue, are those which are subject to only one reflection that are positioned in different part of the image plane depending which mirror meet, those that hit the xy-mirror correspond to the beam elongated along z, the zy-mirror correspond to the beam elongate along x. At the end, the green dots, are the rays that do both reflection and are centred to the center of the image plane by definition of it.

4.2.1 Alignment

Alignment of a beam is important for experimental use so, this section studies the behaviour of a beam when the beam is not perfectly align, in order to understand the behaviour of the beam in the different cases and act consequently.
The parameter that are changed are :

1. orthogonality

2. incidence angle

3. point of incidence

Using a focusing parabolic Montel system with a source of square shape having a side of 1μm, and a Gaussian divergence with FWHM of 25μm

4.2.2 Alignment: Orthogonality

In this section is it done an orthogonality studies of the Montel system, it is studied the behaviour of a beam, using a source parameter defined before. Figure 4.6b presents the interesting histogram versus the horizontal angle x' when the angle between the mirrors change ($\alpha = 90° + \Delta$). It can be noted a improvement of the collimation of the beam changing the angle in the case of closer mirrors ($\Delta = -0.004°$).
Figure show the trend of the FWHM of the x' changing the angle Δ, it is possible to note a minimum for negative angle (this situation correspond to the indigo line) after that the situation become worse. Moreover, the behaviour of the FWHM is not symmetric with respect to $0°$, in case of negative angle deviation the situation improve for small range of deviation angle, after that, the trend get worse, on the opposite way, the situation get worse increasing the positive deviation angle.

4.2.3 Alignment: Incidence angle

To understand the behaviour of a non aligned beam it is simulated the situation of a beam that arrive at the Montel system with the wrong angle. In this particular case the system is defined as follow: incidence angle of 3°, square spot of $100\mu\ m^2$, Gaussian divergence with FWHM of 25μrad. Figure

4.2.4 Alignment: point of incidence

Another way that can be studied to align correctly a beam, is to study the behaviour of a non centred beam with respect to the center of the Montel system.
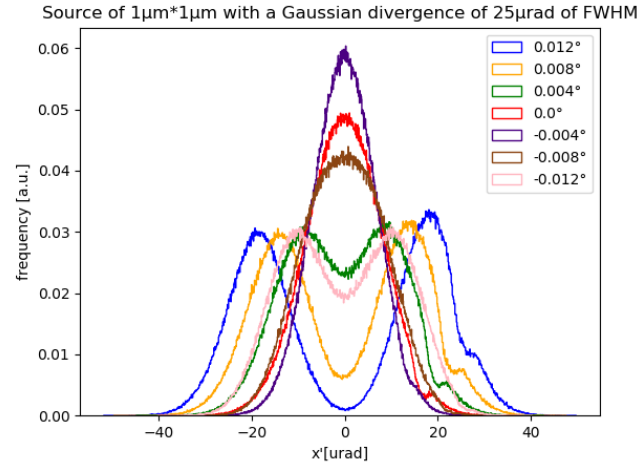
(a) Real histogram
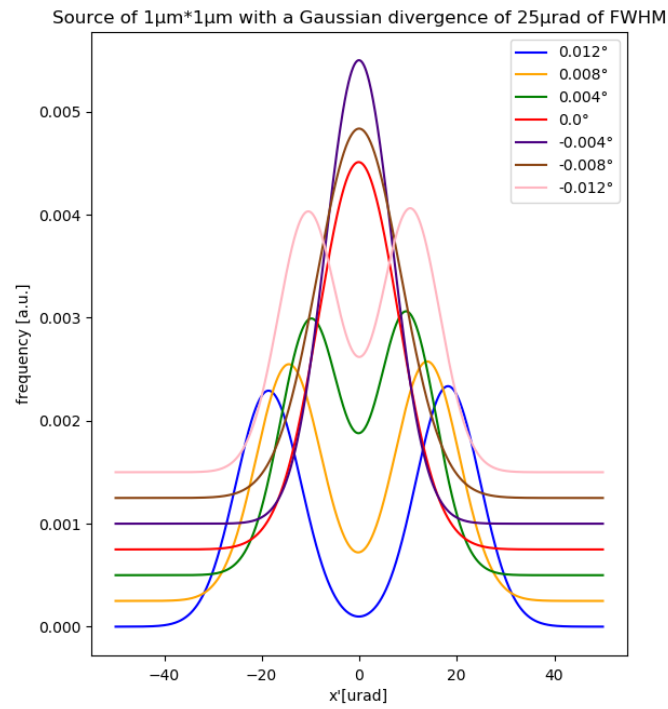
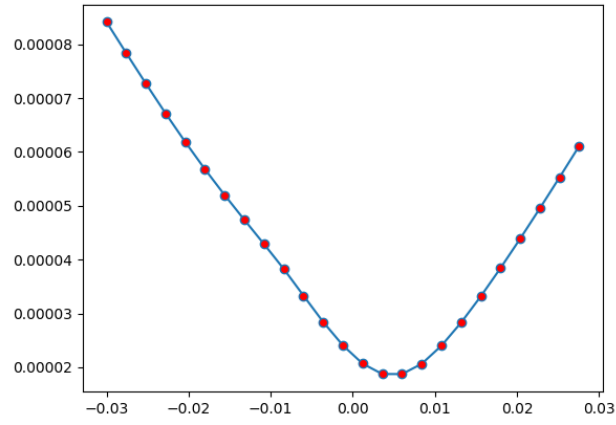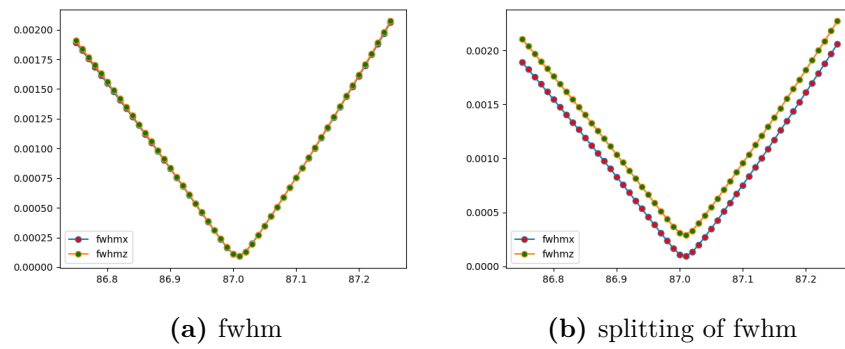**(b)** Fitted Histogram

Figura 4.6: Histogram of x' after Montel

Figura 4.7: FWHM of x' after the Montel changing the orthogonality

(a) fwhm

(b) splitting of fwhm
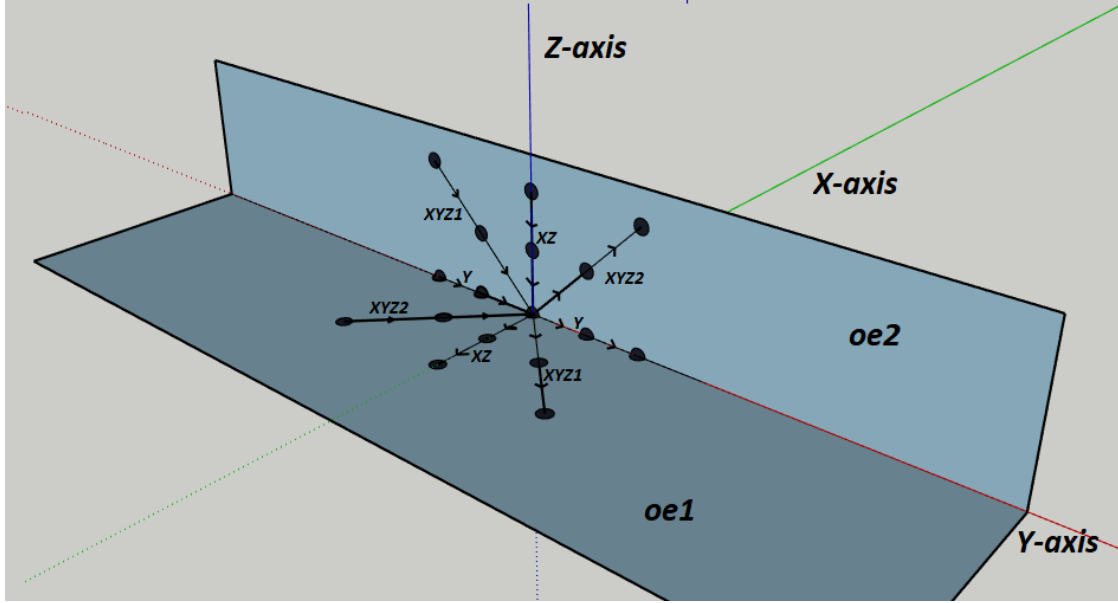
Figura 4.8: Incidence angle

Figura 4.9: Different path for simulate the non-centred beam

In this section is reported the behaviour about the change of FWHM of both x' and z' following different path. Figure 4.9 show the different path followed to simulate the non-centred beam that are named:

1. Y

2. XZ

3. XYZ1

4. XZY2

Figure 4.10 show the behaviour of the two FWHM of the beam changing the incidence point of the beam moving the different paths. This point is defined with respect to the center of the Montel system that correspond to the origin (0, 0, 0). In Figure 4.11a, the incidence point move along y-axis, start from the point (0, 1.5mm, 0) and arriving to the point (0, -1.5mm, 0), and show, more or less, a flat behaviour of the FWHM. Figure 4.11b start from the point (0, 0, 0.15mm) and arrive to (-0.15mm, 0, 0) and have specular behaviour for the two FWHM, there is a minumum of the two FWHM near the origin point, moving on the oe1 worse the FWHM of z' and maintain the other constant, on the contrary, moving on the oe2 the situation is reversed, in this case the FWHM of x' get worse, maintaining constant the one of z'. Figure 4.11c start from (0, 1.5mm, 0.15mm) and arrive to (-0.15mm, -1.5mm, 0) and Figure 4.11d start from (-0.15mm, 1.5mm, 0) and arrive to (0., -1.5mm, 0.15mm). The behaviour of this last two path are similar to that of 4.11b, this is reasonable, because the motion along y-axis does not influence the FWHM because of the definition of the cylindrical mirror, that in any point along the y direction have the same geometry. In Figure 4.11 it is show the intensity profile of the two-reflection beam after the Montel, calculated as the number of the rays in the two-reflection beam with respect to the initial number of rays. The
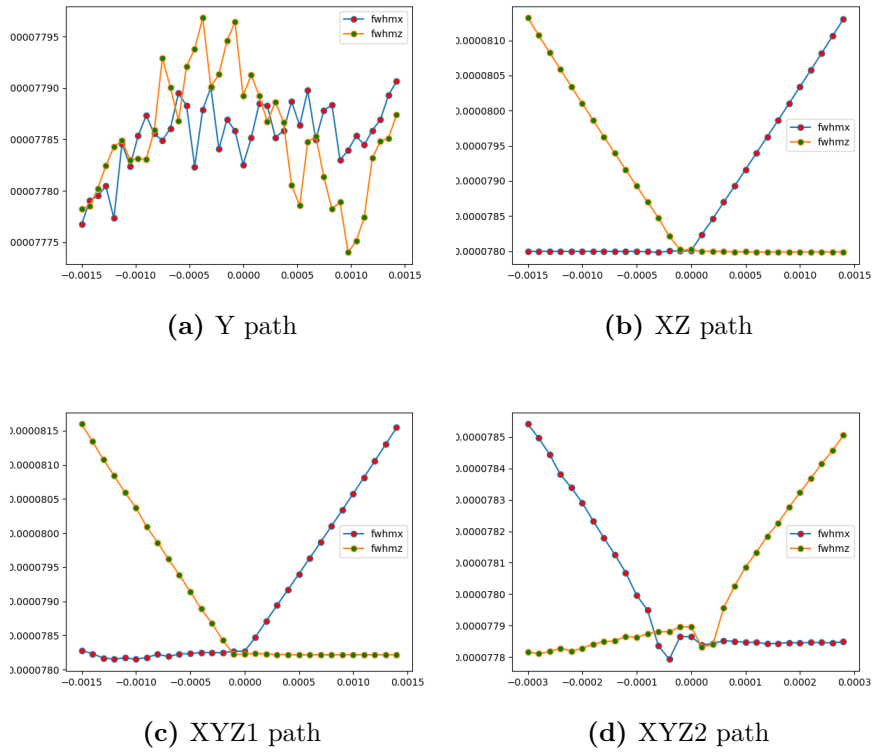
(a) Y path

(b) XZ path

(c) XYZ1 path

(d) XYZ2 path

Figura 4.10: Resuts of the Montel system of a source beam with a FWHM spot of 2.5μm and a Gaussian divergence of $5mrad$

(a) Y path

(b) XZ path

(c) XYZ1 path

(d) XYZ2 path
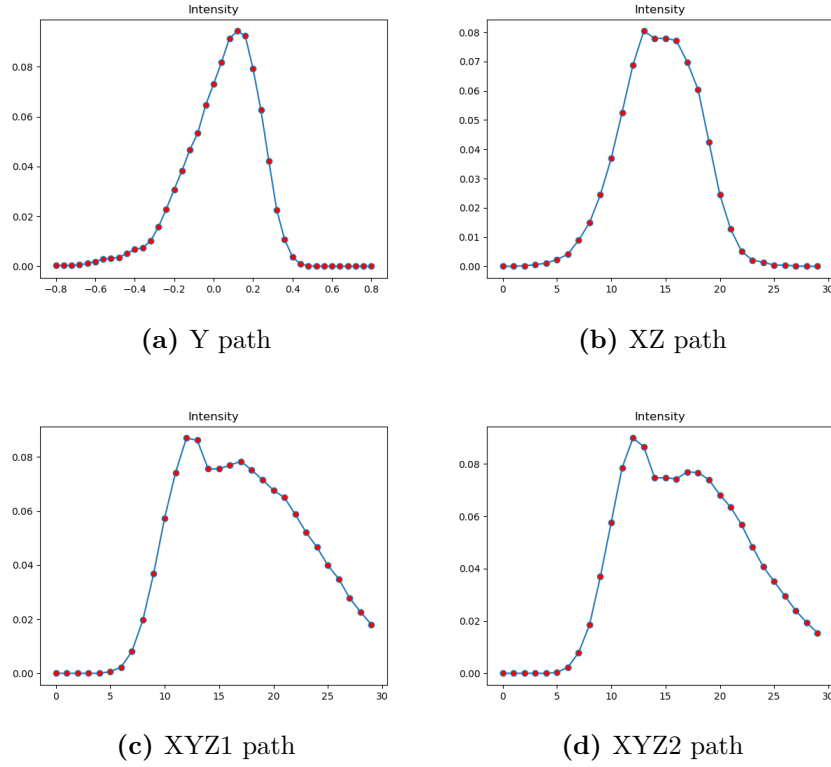
Figura 4.11: Resuts of the Montel system of a source beam with a FWHM spot of 2.5μm and a Gaussian divergence of 5$mrad$

source used, in this case, correspond to a big spot of a square geometry with an area of $1mm^2$, and a large Gaussian divergence with a FWHM of 10mrad. The Montel used is a parabolic localizing system having e an object distance of 1m, an image distance of 3m, an incidence angle of 2° and a finite dimension, with a length of 20cm and a width of 2cm. The different path move along these points; ymax=50cm, ymin=-50cm, xmin=-2cm, xmax=0, zmax=2cm, zmin=0

The plots in Figure 4.11, are interesting, because rappresent the intensity of the "green" Beam in Figure 4.5, that can be directly measured and so, it is possible to realted the centring of the Beam calculating the intensity of this Beam.

Appendice A

Primo Capitolo d'Appendice

Lorem ipsum dolor sit amet, consectetuer adipiscing elit. Ut purus elit, vestibulum ut, placerat ac, adipiscing vitae, felis. Curabitur dictum gravida mauris. Nam arcu libero, nonummy eget, consectetuer id, vulputate a, magna. Donec vehicula augue eu neque. Pellentesque habitant morbi tristique senectus et netus et malesuada fames ac turpis egestas. Mauris ut leo. Cras viverra metus rhoncus sem. Nulla et lectus vestibulum urna fringilla ultrices. Phasellus eu tellus sit amet tortor gravida placerat. Integer sapien est, iaculis in, pretium quis, viverra ac, nunc. Praesent eget sem vel leo ultrices bibendum. Aenean faucibus. Morbi dolor nulla, malesuada eu, pulvinar at, mollis ac, nulla. Curabitur auctor semper nulla. Donec varius orci eget risus. Duis nibh mi, congue eu, accumsan eleifend, sagittis quis, diam. Duis eget orci sit amet orci dignissim rutrum.

Facendo copia–incolla da si può affermare quanto segue: [. . .]Un codice in linea è un frammento di codice appartenente al flusso del discorso, come per esempio `set(0,'DefaultFigureWindowStyle','Docked');`[. . .][. . .]Le prime righe del file pulisci_TESI.m apparirebbero così:

Codice A.1: Inizializzazione di MatLab

```
1  %% Pulizia e Ancoraggio Figure
2  %
3  clear all
4  close all
5  clc
6  %
7  set(0,'DefaultFigureWindowStyle','Docked');
8  %
```

Si può trasformare facilmente un codice in display in oggetto mobile: codice A.2 nella pagina successiva. Lorem ipsum dolor sit amet, consectetuer adipiscing elit. Ut purus elit, vestibulum ut, placerat ac, adipiscing vitae, felis. Curabitur dictum gravida mauris. Nam arcu libero, nonummy eget, consectetuer id, vulputate a, magna. Donec vehicula augue eu neque. Pellentesque habitant morbi tristique senectus et netus et malesuada fames ac turpis egestas. Mauris ut leo. Cras viverra metus rhoncus sem. Nulla et lectus vestibulum urna fringilla ultrices. Phasellus eu tellus sit amet tortor gravida placerat. Integer sapien est, iaculis in, pretium quis, viverra ac, nunc. Praesent eget sem vel leo ultrices bibendum. Aenean faucibus.

Codice A.2: prova

```
1  %% Pulizia e Ancoraggio Figure
2  %
3  clear all
4  close all
5  clc
6  %
7  set(0,'DefaultFigureWindowStyle','Docked');
8  %
```

Morbi dolor nulla, malesuada eu, pulvinar at, mollis ac, nulla. Curabitur auctor semper nulla. Donec varius orci eget risus. Duis nibh mi, congue eu, accumsan eleifend, sagittis quis, diam. Duis eget orci sit amet orci dignissim rutrum.

Codice A.3: prova codice intero

```
1   %% Pulizia e Ancoraggio Figure
2   %
3   clear all
4   close all
5   clc
6   %
7   set(0,'DefaultFigureWindowStyle','Docked');
8   %
9   %commandwindow
10  %
11  %% Modifica Parametri per stesura Tesi
12  %
13  %% AXES
14  %
15  % factoryAxesFontAngle: 'normal'
16  % factoryAxesFontName: 'Helvetica'
17  % factoryAxesFontSize: 10
18  % factoryAxesFontUnits: 'points'
19  % factoryAxesFontWeight: 'normal'
20  %
21  set(0,'DefaultAxesFontSize',16);
22  %
23  %% TEXT
24  %
25  % factoryTextFontAngle: 'normal'
26  % factoryTextFontName: 'Helvetica'
27  % factoryTextFontSize: 10
28  % factoryTextFontUnits: 'points'
29  % factoryTextFontWeight: 'normal'
30  %
```

```
31  set(0,'DefaultTextFontSize',16);
32  %
33  %% LINE
34  %
35  % factoryLineLineStyle: '-'
36  % factoryLineLineWidth: 0.5000
37  %
38  set(0,'DefaultLineLineWidth',1.5);
39  %
40  %% GRID
41  %
42  % factoryAxesGridLineStyle: ':'
43  % factoryAxesMinorGridLineStyle: ':'
44  % factoryAxesXGrid: 'off'
45  % factoryAxesXMinorGrid: 'off'
46  %
47  set(0,'DefaultAxesXGrid','on');
48  set(0,'DefaultAxesYGrid','on');
49  set(0,'DefaultAxesZGrid','on');
50  %
51  set(0,'DefaultAxesGridLineStyle','--');
52  %
53  %% AXIS
54  % axis([xmin xmax ymin ymax])
55  %
56  %% MARKER
57  %
58  % factoryLineMarker: 'none'
59  % factoryLineMarkerEdgeColor: 'auto'
60  % factoryLineMarkerFaceColor: 'none'
61  % factoryLineMarkerSize: 6
62  %
63  % set(0,'DefaultLineMarkerFaceColor','auto');
64  set(0,'DefaultLineMarkerSize',8);
65  %
```

Lorem ipsum dolor sit amet, consectetuer adipiscing elit. Ut purus elit, vestibulum ut, placerat ac, adipiscing vitae, felis. Curabitur dictum gravida mauris. Nam arcu libero, nonummy eget, consectetuer id, vulputate a, magna. Donec vehicula augue eu neque. Pellentesque habitant morbi tristique senectus et netus et malesuada fames ac turpis egestas. Mauris ut leo. Cras viverra metus rhoncus sem. Nulla et lectus vestibulum urna fringilla ultrices. Phasellus eu tellus sit amet tortor gravida placerat. Integer sapien est, iaculis in, pretium quis, viverra ac, nunc. Praesent eget sem vel leo ultrices bibendum. Aenean faucibus. Morbi dolor nulla, malesuada eu, pulvinar at, mollis ac, nulla. Curabitur auctor semper nulla. Donec varius orci eget risus. Duis nibh mi, congue eu, accumsan eleifend, sagittis quis, diam. Duis eget orci sit amet orci dignissim rutrum.

Appendice B

Secondo Capitolo d'Appendice

Lorem ipsum dolor sit amet, consectetuer adipiscing elit. Ut purus elit, vestibulum ut, placerat ac, adipiscing vitae, felis. Curabitur dictum gravida mauris. Nam arcu libero, nonummy eget, consectetuer id, vulputate a, magna. Donec vehicula augue eu neque. Pellentesque habitant morbi tristique senectus et netus et malesuada fames ac turpis egestas. Mauris ut leo. Cras viverra metus rhoncus sem. Nulla et lectus vestibulum urna fringilla ultrices. Phasellus eu tellus sit amet tortor gravida placerat. Integer sapien est, iaculis in, pretium quis, viverra ac, nunc. Praesent eget sem vel leo ultrices bibendum. Aenean faucibus. Morbi dolor nulla, malesuada eu, pulvinar at, mollis ac, nulla. Curabitur auctor semper nulla. Donec varius orci eget risus. Duis nibh mi, congue eu, accumsan eleifend, sagittis quis, diam. Duis eget orci sit amet orci dignissim rutrum.

Nam dui ligula, fringilla a, euismod sodales, sollicitudin vel, wisi. Morbi auctor lorem non justo. Nam lacus libero, pretium at, lobortis vitae, ultricies et, tellus. Donec aliquet, tortor sed accumsan bibendum, erat ligula aliquet magna, vitae ornare odio metus a mi. Morbi ac orci et nisl hendrerit mollis. Suspendisse ut massa. Cras nec ante. Pellentesque a nulla. Cum sociis natoque penatibus et magnis dis parturient montes, nascetur ridiculus mus. Aliquam tincidunt urna. Nulla ullamcorper vestibulum turpis. Pellentesque cursus luctus mauris.

La tabella B.1 nella pagina seguente riporta, con i rispettivi codici identificativi, le prove sperimentali effettuate. . . .

Codice B.1: pollo

```
1  import numpy as np
2
3  a = a + 1
4  b =0
5  for i in arang (a):
6      a = a + i
7
8  print (a)
```

as it is showed in Code B.1

Tabella B.1: Elenco completo delle prove sperimentali. I codici evidenziati indicano le prove che hanno dato buoni risultati.

Codice	Parametro1	Parametro2 [m]	Parametro3 [N]	Opzione1	Opzione2	Opzione3
030	DENTE	1.5	142	NO	–	NO
201	DENTE	1.5	175	NO	–	NO
410	DENTE	1.8	142	NO	–	NO
011	DENTE	1.55	175	NO	–	NO
150	PIEDE	1.5	142	NO	–	NO
161	PIEDE	1.5	98	NO	–	NO
113	PIEDE	1.8	142	NO	–	NO
141	PIEDE	1.55	98	NO	–	NO
1300	DENTE	1.5	142	SI	SI	NO
1201	DENTE	1.5	165	SI	SI	NO
1070	DENTE	1.8	142	SI	SI	NO
1811	DENTE	1.55	165	SI	SI	NO
1106	PIEDE	1.5	142	SI	SI	NO
1501	PIEDE	1.5	98	SI	SI	NO
2110	PIEDE	1.8	142	SI	SI	NO
1411	PIEDE	1.55	98	SI	SI	NO
14110	PIEDE	1.8	142	SI	NO	NO
16210	DENTE	1.8	142	SI	NO	NO
19220	DENTE	1.9	142	SI	NO	NO
10110	PIEDE	1.8	142	SI	NO	NO
11142	PIEDE	1.9	142	SI	NO	NO
712100	PIEDE	1.5	142	SI	NO	SI
112142	PIEDE	1.9	142	SI	NO	SI

Acronimi

CFD   Computational Fluid Dynamics

Computational Fluid Dynamics is a branch of fluid mechanics that uses numerical methods and algorithms to solve and analyze problems that involve fluid flows. Computers are used to perform the calculations required to simulate the interaction of liquids and gases with surfaces defined by boundary conditions.
www.en.wikipedia.org

HPC   High Performance Computing

In informatica con il termine High Performance Computing (calcolo ad elevate prestazioni) ci si riferisce alle tecnologie utilizzate da computer cluster (insieme di computer connessi tra loro tramite una rete telematica) per creare dei sistemi di elaborazione in grado di fornire delle prestazioni molto elevate, ricorrendo tipicamente al calcolo parallelo.
www.it.wikipedia.org

OpenFOAM   Open source Field Operation And Manipulation

The OpenFOAM® CFD Toolbox is a free, open source CFD software package which has a large user base across most areas of engineering and science, from both commercial and academic organisations. OpenFOAM has an extensive range of features to solve anything from complex fluid flows involving chemical reactions, turbulence and heat transfer, to solid dynamics and electromagnetics. It includes tools for meshing, notably *snappyHexMesh*, a parallelised mesher for complex CAD geometries, and for pre- and post-processing. Almost everything (including meshing, and pre- and post-processing) runs in parallel as standard, enabling users to take full advantage of computer hardware at their disposal.
www.openfoam.com

CINECA   Consorzio Interuniversitario per il Calcolo Automatico

Cineca è un Consorzio Interuniversitario senza scopo di lucro formato da 69 università italiane e 3 Enti. Costituito nel 1969, oggi il Cineca è il maggiore centro di calcolo in Italia, uno dei più importanti a livello mondiale. Operando sotto il controllo del Ministero dell'Istruzione dell'Università e della Ricerca, offre supporto alle attività della comunità scientifica tramite il supercalcolo e le sue applicazioni, realizza sistemi gestionali per le amministrazioni universitarie e il MIUR, progetta e sviluppa sistemi informativi per pubblica amministrazione, sanità e imprese.
www.cineca.it

Bibliografia

[RKM15] Giacomo Resta, Boris Khaykovich, and David Moncton. Nested kirkpatrick–baez (montel) optics for hard x-rays. *Journal of Applied Crystallography*, 48(2):558–564, 2015.